© 2015. Published by The Company of Biologists Ltd | Development (2015) 142, 1960-1970 doi:10.1242/dev.118448

RESEARCH ARTICLE

STEM CELLS AND REGENERATION

Essential elements for translation: the germline factor Vasa functions broadly in somatic cells

Mamiko Yajima* and Gary M. Wessel

ABSTRACT

Vasa is a conserved RNA-helicase found in the germ lines of all metazoans tested. Whereas Vasa presence is often indicated as a metric for germline determination in animals, it is also expressed in stem cells of diverse origin. Recent research suggests, however, that Vasa has a much broader function, including a significant role in cell cycle regulation. Results herein indicate that Vasa is utilized widely, and often induced transiently, during development in diverse somatic cells and adult precursor tissues. We identified that Vasa in the sea urchin is essential for: (1) general mRNA translation during embryogenesis, (2) developmental re-programming upon manipulations to the embryo and (3) larval wound healing. We also learned that Vasa interacted with mRNAs in the perinuclear area and at the spindle in an Importin-dependent manner during cell cycle progression. These results suggest that, when present, Vasa functions are essential to contributing to developmental regulation.

KEY WORDS: Vasa, Wound healing, Multipotent cells, Cell-cycle regulator, Sea urchin, Translation

INTRODUCTION

Vasa is expressed in germ cells of all metazoans tested (Hay et al., 1988; Lasko and Ashburner, 1988, 1990; Raz, 2000; Yajima and Wessel, 2011a), yet recent studies demonstrate that Vasa has much broader functional roles in stem cells, cancer cells and in somatic embryonic cells (Rebscher et al., 2007; Janic et al., 2010; Yajima and Wessel, 2011b,c; Lasko, 2013; Juliano and Wessel, 2010; Paz-Gómez et al., 2014; Schwager et al., 2014). However, its function in these diverse cells remains unclear, especially when considering different demands between the germ line and somatic lineages. We previously reported in the sea urchin embryo that Vasa localized to the spindle in early blastomeres during M phase and functioned in cell cycle progression during embryogenesis, in addition to its roles in the germ line (Yajima and Wessel, 2011b,c). A similar cell cycle function was reported in *Drosophila* germline stem cells (Pek and Kai, 2011), and these results cast new light onto Vasa as a regulator of cellular potency in proliferative cells.

Echinoderms are a sister group to chordates and are known for their strong regenerative abilities. Representatives of each of the major groups of echinoderms can regenerate entire body segments as an adult, complete with skeletons, neurons and gravid gonads (e.g. Goss, 1969; Emson and Wilkie, 1980; Mashanov and García-Arrarás, 2011). Echinoderm larvae can even produce a functional larval clone derived by budding from the original larval body (Bosch et al., 1989; Eaves and Palmer, 2003). Embryos from this phylum are well known for marked regulative development; many cells maintain 'multipotency' and change fates in response to changes in neighbouring cells (Horstadius, 1950,1973; Ransick and Davidson, 1993; Dubois and Ameye, 2001), including the germ line (Goss, 1969; Emson and Wilkie, 1980; Eaves and Palmer, 2003; Vaughn and Strathmann, 2008; Ransick and Davidson, 1993).

Sea urchins have only one *vasa* gene (Voronina et al., 2008). The authenticity of this gene as *vasa* was previously documented and it is highly conserved, especially in the DEAD box and C-terminal domains (Juliano et al., 2006; Juliano and Wessel, 2009; Gustafson and Wessel, 2010a,b). During early sea urchin development, *vasa* mRNA is uniformly distributed throughout the early embryo, and after gastrulation it becomes enriched in the small micromere lineage. Vasa protein is also uniformly distributed until the 8-cell stage, but becomes enriched in the micromeres at the 16-cell stage and then in the small micromeres at the 32-cell stage (Voronina et al., 2008). Although the *vasa* mRNA and the Vasa protein are both concentrated in the small micromere lineage, they are both detectable throughout the embryo and larva. In this report, we reveal broad functional contributions and unique regulatory mechanisms used by Vasa outside of the germ line that are essential for the developmental plasticity of the embryo, a function that might be widely conserved among other organisms.

RESULTS

Vasa is expressed in multiple cell lineages during development

Vasa is expressed throughout the egg and the early blastomeres of the sea urchin *Strongylocentrotus purpuratus*, and becomes enriched in the small micromere descendants that give rise to the germ line upon their formation (Voronina et al., 2008; Yajima and Wessel, 2011a). Vasa accumulation is expanded significantly to include the coelomic pouches, especially in the left side, where the adult rudiment is formed in the late larval stage (Fig. 1A,E; compare Vasa distribution of the left and right coelomic pouches between day-3 and day-5 larvae). Although a detailed lineage map of all cellular origins of the coelomic pouch is not yet known, contributions to this tissue come from small micromere and macromere descendants (e.g. Cameron et al., 1991) (Fig. 1F and Table 1). Additional contribution comes from the amniotic invagination of the ectoderm, which extends to and merges with the coelomic pouches to form an adult rudiment in the late larval stage (Fig. 1B-D, summarized in Fig. 1F and Table 1) (Cameron et al., 1987, 1991). The fidelity of Vasa labelling in this approach has been previously reported and includes use of the same controls and affinity-purified antibodies here (e.g. Voronina et al., 2008; Juliano and Wessel, 2009; and data not shown). At present, it is unknown what regulates Vasa expression in these late larvae, but recent work (Materna et al., 2013) suggests that the transcription

MCB Department, Brown University, 185 Meeting Street, BOX-GL173, Providence, RI 02912, USA.

*Author for correspondence (Mamiko_Yajima@brown.edu)

Received 5 October 2014; Accepted 30 March 2015

Development (2015) 142, 1960-1970 doi:10.1242/dev.118448

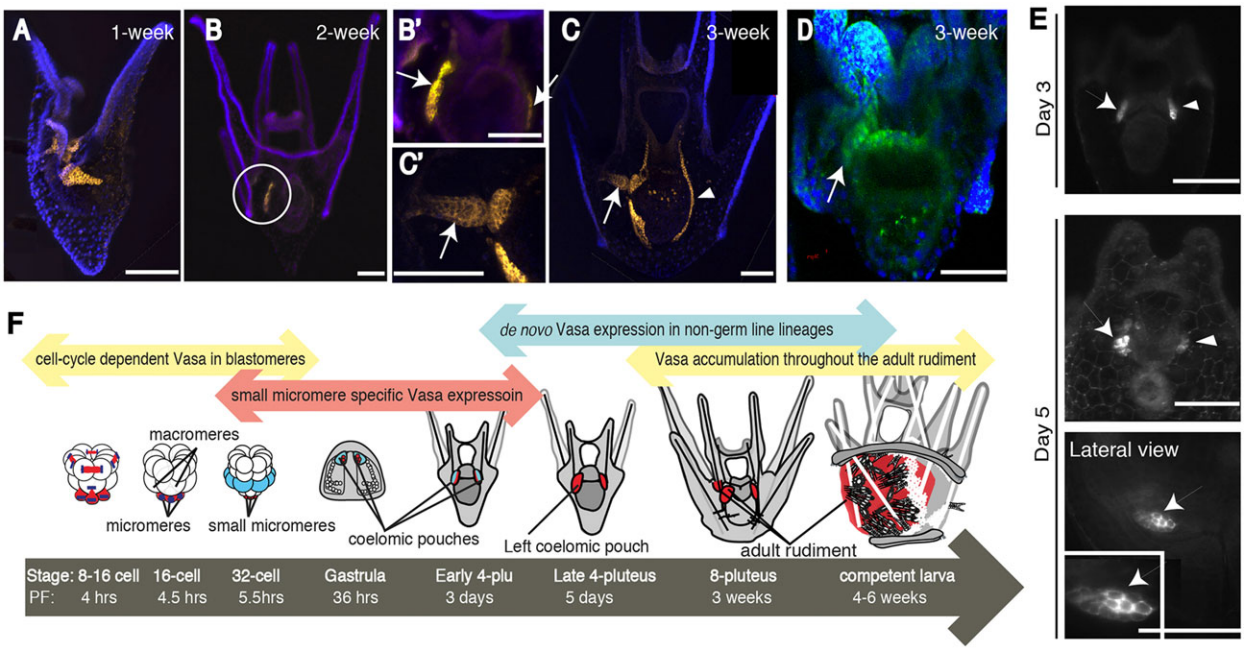

Fig. 1. Transient expression of Vasa arises from multiple lineages during development of *S. purpuratus* larvae. (A-C) Confocal *z*-stack images of Vasa immunostaining (yellow) at 1 week (A), 2 weeks (B) and 3 weeks (C) post fertilization, counterstained by Hoechst (blue). Vasa is initially enriched in the small micromeres and then expands throughout the coelomic pouches, which include macromere and mesomere lineages, approximately from day 5-7 larvae (A, also see E). The Vasa signal further expands into invaginating tissue derived from the ectoderm at the onset of the amniotic invagination to form an adult rudiment (C,D). B′ and C′ are higher magnification views of B and C, respectively. B′ indicates Vasa$^+$ cells expanded in the entire coelomic pouches. Arrow in C′ indicates Vasa$^+$ invaginating tissue. (D) A confocal *z*-stack image of vasa mRNA (green) localization in the adult rudiment (arrow) by *in situ* hybridization counterstained by Hoechst (blue). (E) Vasa signal was symmetrically distributed in the left (arrow) and right (arrowhead) coelomic pouches (day 3), yet the signal in the left became more intensive from day 5 onwards. In those larvae, two layers of Vasa$^+$ cells were often found following day 5: one layer with stronger Vasa expression than the other (bottom panel, arrow). The inset is the higher magnification view of the single left coelomic pouch. Larvae were immunolabelled by anti-Vasa antibody. Images were taken by fluorescent microscopy. (F) Summary diagram of Vasa expression during development observed in this report or in previous studies. A transient Vasa expression occurs in various cell lineages during development. Vasa (Red) is expressed in the egg, embryonic cells, PGCs, adult rudiment cells and tissues in wound healing. PF, post fertilization. Scale bars: 50 µm.

factor FoxY controls the multipotency of coelomic pouch cells, and that, in turn, FoxY is activated by Delta/Notch signalling, beginning in the 16-cell stage.

To directly test here whether the expanded Vasa accumulation in the coelomic pouch is entirely derived from the small micromere lineage, several approaches were taken. First, the Vasa$^+$ micromeres/small micromeres were surgically depleted at the 16- and 32-cell stages of *L. variegatus* embryos. This species was used only for this experiment because the embryo exhibits relatively little compensatory Vasa upregulation throughout the embryo compared with *S. purpuratus* (Voronina et al., 2008). This feature of the embryo makes for a more robust lineage conclusion, especially during the process of developmental recovery (referred to here as developmental re-programming). Following micromere and small-micromere removal, Vasa$^+$ cells were not detected during early development in these embryos (Yajima and Wessel, 2011a). However, new Vasa$^+$ cells reappeared in the coelomic pouches of the late feeding larvae (supplementary material Fig. S1A), similar to the original signal in wild-type larvae. This supports the conclusion of an additional, non-micromere lineage for this Vasa expression in the coelomic pouch. Next, we tested in *S. purpuratus* whether the macromere descendants (the tier of cells adjacent to the micromeres, thought to contribute to the coelomic pouch) became Vasa$^+$ in normal embryos by injecting a reporter *vasa-GFP* mRNA (Gustafson et al., 2011) into fertilized eggs and a fluorescent dye into a single macromere of the 16-cell embryo (supplementary material Fig. S1B). The reporter Vasa-GFP approach is of high fidelity in reflecting endogenous Vasa expression, and it allows for longitudinal analysis of individual embryos (Gustafson et al., 2011). The macromere descendants and the Vasa-GFP$^+$ cells did not overlap early in development (supplementary material Fig. S1B, day 3, arrows), but did so during larval development; ∼15% of the macromere descendants in the coelomic pouch expressed Vasa-GFP (supplementary material Fig. S1B, day 5, arrows). Previous studies documented a strict Vasa regulation by post-translational degradation – *vasa* mRNA is ubiquitously present until gastrula stage and is translated in all cells of the early embryo and larva, but is degraded rapidly in all cells except the germ cells (Gustafson et al., 2011; Yajima and Wessel, 2011b). Thus, the accumulation of Vasa in macromere descendants in the larva, which were previously Vasa-less cells, demonstrated a definitive somatic and post-transcriptional regulation of Vasa, consistent with the presence and dynamics of endogenous Vasa (Fig. 1; supplementary material Fig. S2).

High levels of Vasa accumulation continued during pouch development and throughout the adult rudiment (supplementary material Fig. S2A-E), together with lower amounts in the mouth and intestine of the larva. These tissues were also labelled by the affinity-purified anti-Vasa antibody (Voronina et al., 2008) and demonstrated a non-germline lineage for Vasa expression. The functional contributions of Vasa in those tissues are unclear, yet, considering that the left coelomic pouch originally consisted of about ten cells (Cameron et al., 1987, 1991), the amount of cell proliferation and Vasa expression in the adult rudiment is significant. Interestingly, these pouch cells also expressed *seawi* (a *piwi* orthologue in the sea urchin) and the positive cell cycle

Development (2015) 142, 1960-1970 doi:10.1242/dev.118448

Table 1. Vasa expression during development observed in this report or in previous studies. A transient Vasa expression occurs in various cell lineages during development.

	16-cell	Blastula	Gastrula	4-pluteus	8-pluteus	Competent larva
Endogenous Vasa protein	++ in micromeres <>: Every cell	++ in micromeres + in every cell	++ in micromeres + in every cell	++ in coelomic pouches + in mouth & intestine +/– in every cell	++ in adult rudiment + in mouth & intestine +/– in every cell	↓ in adult rudiment + in mouth & intestine +/– in every cell
Endogenous Vasa mRNA	Every cell	Every cell	++ in micromeres Every cell +	++ in coelomic pouches + in mouth & intestine +/– in every cell	++ in adult rudiment + in mouth & intestine +/– in every cell	↓ in adult rudiment + in mouth & intestine +/– in every cell
Vasa-GFP protein	++ in micromeres <>: Every cell	++ in micromeres + in every cell	++ in micromeres+ in every cell	++ in coelomic pouches + in mouth & intestine +/– in every cell	–	–
Vasa-GFP mRNA	Every cell	Every cell	++ in micromeres + in every cell	++ in coelomic pouches + in mouth & intestine +/– in every cell	–	–

Key: ++, enriched; +, low level; +/–, background level; –, undetectable; <>, spindle; ↓, reduction of signal.

regulator *cyclinB* (supplementary material Fig. S2F-J). Further, these Vasa$^+$ cells have higher BrdU incorporation (DNA synthesis during the cell cycle; see supplementary material Fig. S3A) than Vasa-null cells, suggesting a proliferative state of the Vasa$^+$ somatic cells in the adult rudiment. It should be noted that cells in the mouth and intestine also showed strong BrdU incorporation and is consistent with the link between Vasa expression and the proliferative state of the cells. We conclude that Vasa expression is broad, often transient, in multiple, independent cell lineages from each germ layer, and is associated with increased cell proliferation.

Vasa functions in developmental re-programming and in wound healing

We hypothesized that Vasa might function in increased cellular proliferation, and we designed an experimental protocol to induce rapid cell cycling in otherwise slowly dividing cells to test this hypothesis. Cells in the arms of one-week-old control larvae demonstrate slow cell cycling and near-background levels of Vasa accumulation. However, when we induced physical damage with a glass needle in this quiescent tissue (Fig. 2A) and then pulse-treated with BrdU, we noted an increase in BrdU$^+$ cells throughout the affected areas (Fig. 2B). The density of BrdU$^+$ cells increased ~twofold in the area of injury compared with the same area of uninjured larvae (Fig. 2C), or in non-injured arms of the experimental animals. This suggests a rapid induction of cell proliferation during wound healing in response to the damage. Interestingly, when these BrdU-labelled larvae were tested with the affinity-purified anti-Vasa antibody, endogenous Vasa expression was readily detected in the BrdU$^+$ regions of the damaged larvae (Fig. 2D), but not in similar areas of normal larvae, or in uninjured arms of the damaged larva. Thus, Vasa accumulation is induced to increase rapidly and substantially in cells induced to proliferate.

To test Vasa induction in wound healing with a second approach, *S. purpuratus* day-5 larvae containing *vasa-GFP* mRNA were laser-bleached to damage a subset of larval tissues that do not normally accumulate Vasa protein. Membrane-mCherry mRNA was introduced with Vasa-GFP mRNA to visualize outlines of the cells and to normalize the Vasa-GFP signal in those larvae before and after damage. We detected a ~four- to fivefold increase in Vasa-GFP signal (normalized to membrane-mCherry signal in the same region) in the damaged area (supplementary material Fig. S3B). In this experiment, mRNA (not a transgene) was injected into fertilized eggs, where it spread equally among the progeny, so any Vasa-GFP expression in this experiment was the consequence of post-transcriptional regulation of Vasa-GFP mRNA. Currently, we do not know whether this increase in Vasa signal is a result of increased translation of Vasa, a decrease in Vasa degradation (from a constitutive Vasa translation, as it occurs in the early embryo), or both. It is likely that many new genes were activated for wound healing, potentially including the *cyclins* and other genes involved in cell proliferation, but what is significant here is that Vasa protein is induced to accumulate coincidently with an increase in cellular proliferation.

To explore Vasa induction further, one half of a *S. purpuratus* larva was damaged, and we found that endogenous Vasa accumulation increased over fourfold compared with that of controls (supplementary material Fig. S4A,B). Only a slight increase was observed in mRNA expression by quantitative RT-PCR, and some expansion in spatial expression of Vasa was detected by *in situ* hybridization (supplementary material Fig. S4C,D). We conclude that Vasa protein overexpression is induced in response to tissue damage and occurs primarily post-transcriptionally. This increase is correlated with rapid cell cycling and in damage response of the normally Vasa-less somatic cells.

Next, we functionally tested the contribution of Vasa protein in the wound-healing process. Vasa was knocked down by morpholino antisense oligonucleotide (MO) treatment (supplementary material Fig. S4E). In larvae, *vasa* mRNA was present at near background levels throughout the entire embryo but was enriched in the small micromere lineage (Voronina et al., 2008). One half of an *S. purpuratus* embryo (day 1.5, blastula stage) was damaged by a glass needle during this experiment. Normal embryos that were damaged (normal, Fig. 3A,B) quickly healed their epithelium within 15 min-2 h, recovered swimming phenotypes, and most (80%) of the embryos gastrulated successfully within 20 h of damage. Embryos diminished in Vasa were still capable of development, although they

Development (2015) 142, 1960-1970 doi:10.1242/dev.118448

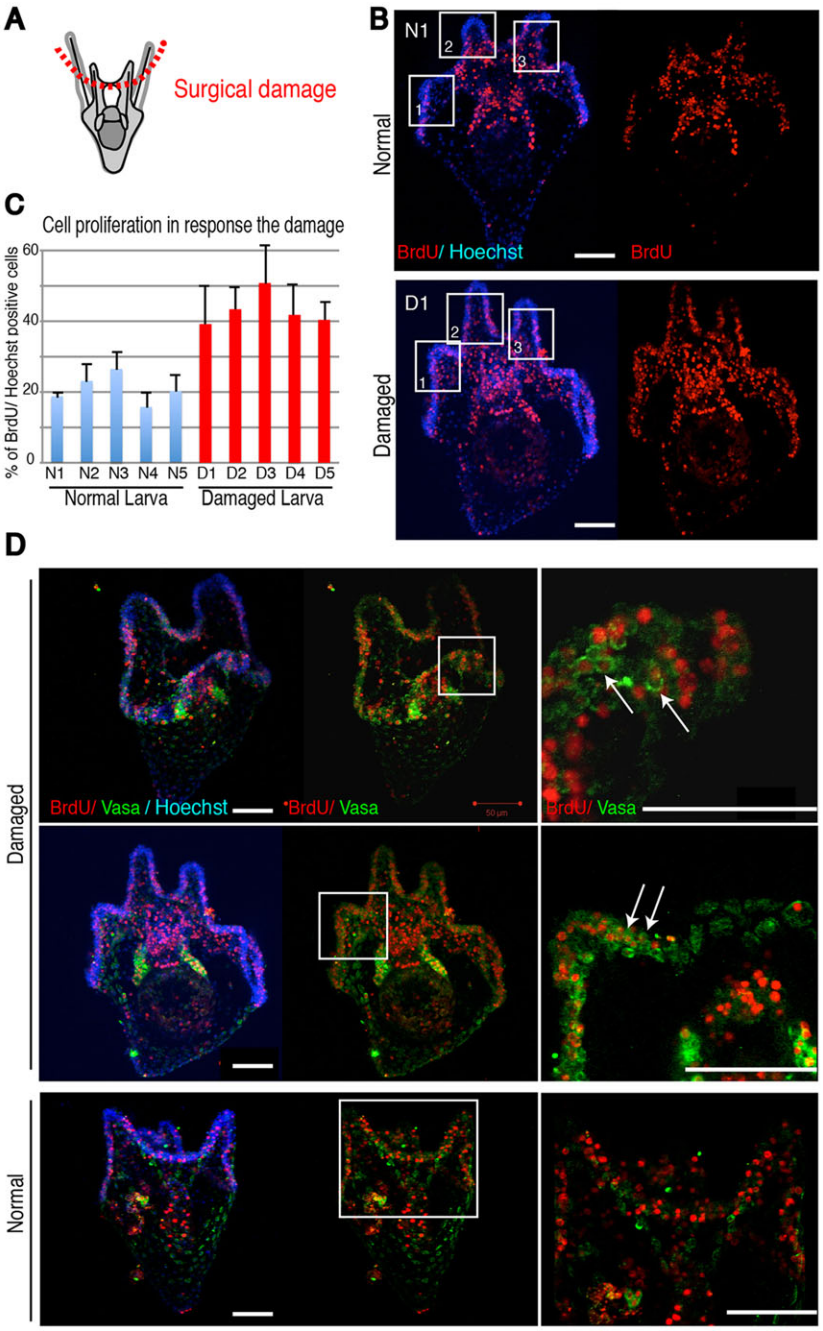

Fig. 2. Rapid cell division and ectopic Vasa expression is induced in response to damage in *S. purpuratus* larvae. Images were *z*-stack projection taken by confocal microscopy. (A) Larval arms were damaged by sliding a glass needle across them. Dashed line indicates a damaged region. (B) Control (N1) and damaged (D1) larvae were treated with 1 µM BrdU for 1 h, stained with anti-BrdU antibody (red) and counterstained with Hoechst (blue). Damaged larvae showed a larger number of $BrdU^+$ cells. Squares 1-3 indicate regions that were counted for percentage of $BrdU^+$ cells per Hoechst signal. The average value obtained from each of normal (N1-5) or damaged (D1-5) larvae is summarized in C. (C) The average percentage of $BrdU^+$ cells per Hoechst signal in each square in B was calculated among three regions per larva, five larvae each from normal (N1-N5) and damaged (D1-D5) larval populations. Cell numbers were counted by ImageJ. (D) Damaged larvae (upper two panels) showed ectopic Vasa expression (green, arrows) on damaged larval arms together with BrdU incorporation (red) that was not observed in normal larva (lower panel). White squares indicate an enlarged region on the right hand of each panel. Scale bars: 50 µm.

lacked the enriched germline Vasa. However, damaged embryos lacking Vasa (Vasa-MO, Fig. 3A,B) were much less capable of repair and recovery; these embryos exhibited significant delays in ectodermal closure, they never resumed swimming or gastrulation and, eventually, they ceased development.

To test the effect of a different developmental stress, we removed micromeres, the major organizer of the embryo, from Vasa-deficient *S. purpuratus* embryos and tested the recovery of the germ line (Fig. 3C) (Yajima and Wessel, 2011a). The resultant embryos were, however, never capable of reaching gastrulation and instead died within 3-4 days after fertilization. On the contrary, Vasa-deficient embryos with micromeres, or embryos lacking micromeres but containing Vasa protein, successfully developed and gastrulated (albeit with some initial delay in development). These results suggest that Vasa is essential for developmental re-programming of the embryo and for wound healing.

Vasa is essential for protein synthesis in the early embryo

We tested the function of Vasa in early embryos and found that Vasa is essential for both reporter (injected mRNAs) and endogenous protein synthesis (Fig. 4A-E). Vasa-GFP mRNA (green) was injected into *S. purpuratus* fertilized eggs, and the Vasa-MO (experimental) or the Nanos2-MO (Nanos2 is another germline marker and used here as a specificity control; see Juliano et al., 2010) was injected into one of the two sibling blastomeres (co-injected with Red Dextran to follow the cell lineage) at the 2-cell stage. The injected embryos were then cultured until the 16- to 32-cell stage (prior to Nanos2 expression) and analysed for both developmental progression as well as expression of the GFP reporter. Injection of Vasa-MO (0.5 mM stock) into one of the 2-cell stage blastomeres resulted in a delay in cell cycle progression in the lineage containing the Vasa-MO (Fig. 4B, Vasa-MO only, arrow)

Development (2015) 142, 1960-1970 doi:10.1242/dev.118448

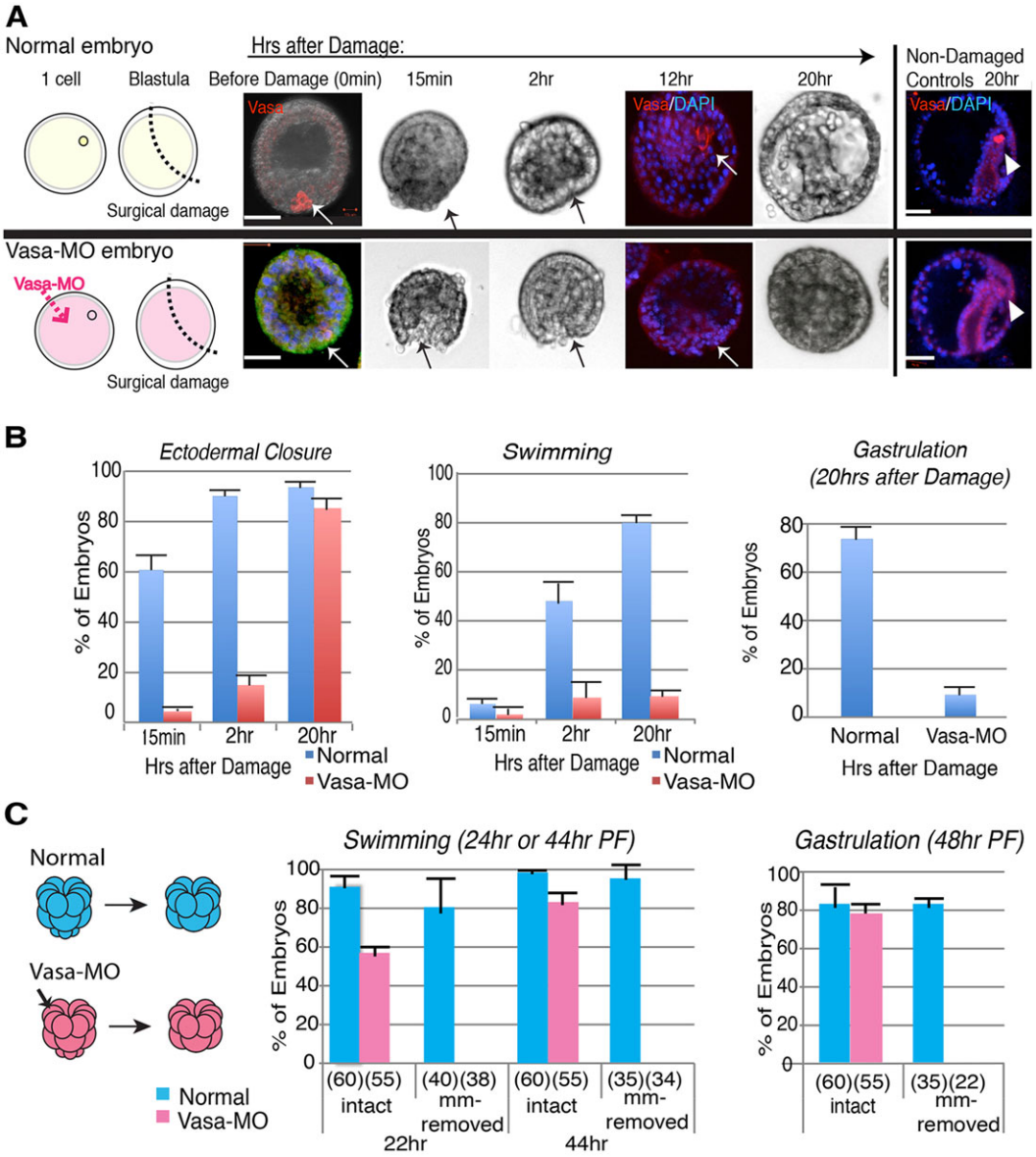

Fig. 3. Vasa is required for wound healing and developmental re-programming. Vasa functionality in cell cycling is dosage dependent (Yajima and Wessel, 2011b), and the amount of Vasa-MO (0.5 mM stock) used here knocked down Vasa^{+} cells in the small micromere lineages, yet cell cycling progressed on time. Fluorescence images were taken by confocal microscopy. (A,B) Embryos were either uninjected (normal) or injected with Vasa-MO at 1-cell stage, and surgically damaged by a glass needle (indicated by a dashed line) at blastula stage (diagram). The damage was performed on one randomly selected half of the embryo. The developmental recovery of each sample was observed either by morphology and/or by Vasa immunofluorescence. Normal day 1.5 embryos recovered from the damage within 2 h and gastrulated successfully within 20 h after damage. Vasa-MO (0.5 mM stock)-injected embryos were incapable of recovering from damage and failed to gastrulate. The MO remains inhibitory for at least 3-4 days following injection. Arrows indicate the vegetal plate area. Arrowhead in non-damaged control indicates normal or Vasa-MO embryos with no surgical damage. Vasa^{+} small micromere was absent in the Vasa-MO-injected embryo at gastrula stage, demonstrating the specificity of Vasa-MO knockdown. (C) Micromeres were removed at 16-cell stage of the normal (blue) or Vasa-MO-injected embryo (red). The resultant embryos reduced in Vasa failed in swimming (24 h PF) and gastrulation (48 h PF) and eventually died. () indicates total number of embryos that were tested. Error bars indicate s.d. of three independent experiments. Scale bar: 50 µm.

(see Yajima and Wessel, 2011b for the detailed phenotype), but not in the sibling lineage. However, when Vasa-GFP (lacking the MO-site) was first injected into the egg, and subsequently the Vasa-MO (recognizing the endogenous but not the reporter Vasa) was injected into one of the 2-cell stage blastomeres, the Vasa-MO-containing blastomere was significantly rescued in development. They succeeded in the asymmetric cellular divisions at the 16-cell stage, even though Vasa-GFP synthesis was reduced by ~30% compared with the control due to a general reduction of translation in those cells (Fig. 4C). Vasa-MO injected lineages showed a similar reduction in Vasa-GFP as well as Ne-GFP (eGFP with a nuclear localization signal) fluorescence, whereas Nanos2-MO-injected cells showed no reduction in the GFP signal (Fig. 4D,E). Although Vasa might have an additional, direct function in cell cycle regulation, these results suggest that Vasa controls cell cycle progression at least partly by regulation of general protein synthesis.

We then tested more generally which protein synthesis is dependent on Vasa function. To address this issue, we incorporated radioactively labelled amino acids into the analysis to identify Vasa-dependent protein synthesis. We injected

Development (2015) 142, 1960-1970 doi:10.1242/dev.118448

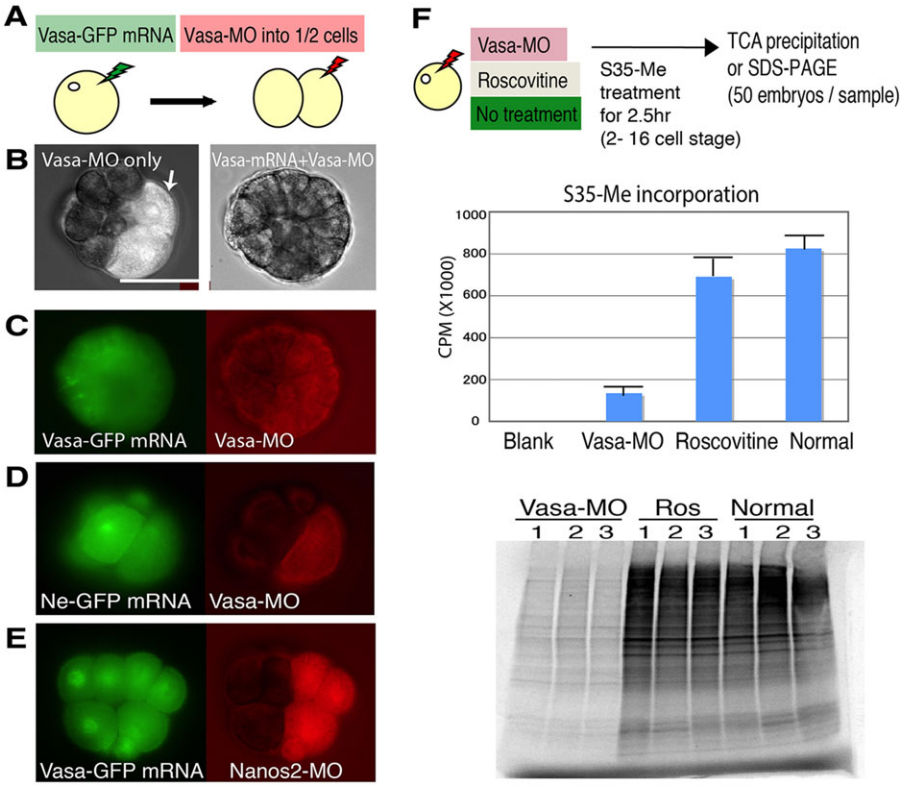

Fig. 4. Vasa is essential for general translational regulation. (A) Experimental procedure. Vasa-GFP mRNA (green) was injected into fertilized eggs and the Vasa- or Nanos2-MO (red) was injected into one of the sibling blastomeres at the 2-cell stage. Embryos were then cultured until the 16- to 32-cell stage. (B-E) Injection with Vasa-MO (0.5 mM stock) into one of the 2-cell-stage blastomeres resulted in a delay in cell cycle progression in the lineage containing the Vasa-MO only (Vasa-MO only, arrow). When Vasa-GFP mRNA was first injected into the egg, and subsequently the Vasa-MO was injected into one of the 2-cell stage blastomeres, the Vasa-MO-containing blastomere was rescued in development (B), even though the Vasa-GFP synthesis was reduced by ~30% (by signal intensity calculation with ImageJ) from the control due to general reduction of translation in those cells (C). Vasa-MO-injected cells showed ~30% reduction (by signal intensity calculation with ImageJ) in Vasa-GFP or Ne-GFP (eGFP with nuclear localization signal) (D) fluorescence, whereas Nanos2-MO-injected cells showed no reduction in the signal (E). Images were taken by fluorescent microscopy. (F) Fertilized eggs injected with Vasa-MO (1 mM stock), treated with roscovitine (a Cdk inhibitor) or uninjected, were incubated with ^{35}S-Met for 2.5 h from 2- to 16-cell stage. Vasa-MO-injected embryos showed ~80% reduction in general translation for ^{35}S incorporation, whereas roscovitine-treated embryos showed little reduction compared with normal embryos. Error bars indicate s.d. of three independent experiments. Scale bar: 50 µm.

S. purpuratus fertilized eggs with the Vasa-MO (1 mM stock) and then incubated the resultant embryos with ^{35}S-methionine for 2.5 h from the 2- to 16-cell stage. Alongside this test, other cohorts of sibling embryos were treated with roscovitine or were untreated. Roscovitine was selected here as a comparison, as it is a cell cycle inhibitor (inhibiting cdk1, 2 and 5 with greatest specificity). As we anticipate that Vasa depletion will result in reduced cell cycling, we wanted to compare levels of protein synthesis in cells blocked from cycling and to distinguish these effects from any Vasa effects independent of cell cycling. Following the incubation period, the same number of embryos from each sibling cohort was split for measuring overall radioactive incorporation, both by TCA precipitation, and by PAGE separation followed by autoradiography. In both types of analysis, Vasa-depleted embryos showed significantly less overall protein synthesis (<20%) relative to both the control cohort and to the roscovitine-treated embryos (Fig. 4F). Although roscovitine treatment inhibited cell cycle progression (data not shown), the amount of overall protein synthesis in these embryos was not significantly different from control embryos (~10% reduction). Thus, cell cycle inhibition did not adversely affect general protein synthesis. Importantly, PAGE analysis of newly synthesized proteins showed that Vasa functions broadly in protein synthesis – of the large numbers of distinct ^{35}S-methionine-labelled proteins detected in control embryos, they were each uniformly decreased in intensity in embryos lacking Vasa (Fig. 4F). This is consistent with the results from TCA precipitation measuring total amino acid incorporation. Thus, Vasa appears to be involved in general protein synthesis in these early embryos, including both the wide population of native proteins as well as exogenously constructed proteins not normally present in these embryos.

Vasa appears to be essential for broad translational regulation, yet it is formally possible that Vasa only interacts with a very limited set of RNAs that encode key translational regulators. Absence of Vasa then might limit translation of this key factor(s) and the whole of translation might then be halted. To determine how broadly the population of mRNA is that interacts with Vasa, we performed Vasa-RIP (immunoprecipitation of RNA associated with Vasa) at 4- to 8-cell or 8-cell stage of *S. purpuratus* embryos. We extracted the mRNA that co-immunoprecipitated with Vasa, and compared it with control RIP results that included specific antibodies to eIF4E and Nanos2 (supplementary material Fig. S5A,B): eIF4E is a general translational regulator by functioning as the 7-methyl-guanosine cap-binding protein of mRNAs and serves as a positive control for broad mRNA association [reviewed by Topisirovic et al. (2011)]. Nanos2, on the other hand, interacts with specific mRNAs through the pumilio response element [reviewed by Saga (2010)] and is rare in embryos of this developmental stage (Juliano et al.,

Development (2015) 142, 1960-1970 doi:10.1242/dev.118448

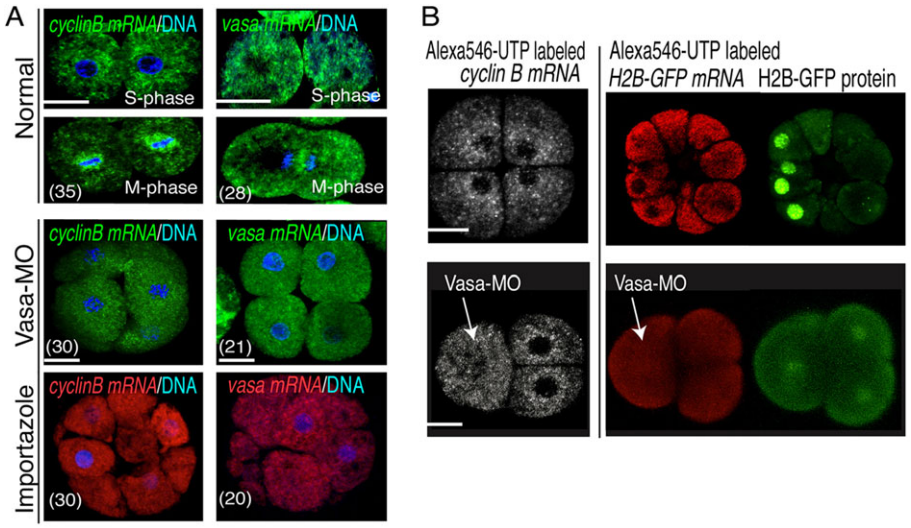

Fig. 5. Vasa-interacting mRNAs show characteristic localization around the spindle during cell cycle progression. (A) *In situ* hybridization images of *cyclinB* or *vasa* mRNAs. mRNAs were localized around the spindle (M phase) and nuclear envelope (S phase) in normal embryo, yet its specific localization was diminished in Vasa-MO (0.5 mM stock)-injected or importazole (importin inhibitor)-treated embryos. () indicates the number of embryos observed. (B) Live imaging of *cyclinB* or *H2B* (*Histone 2B*, DNA marker)-*GFP* mRNAs labelled by Alexa 546-UTP. Labelled mRNAs were injected into the fertilized eggs (upper panels) or into one of the 2-cell-stage embryos. *cyclinB* mRNA demonstrated a perinuclear and spindle localization during cell cycling, whereas the *H2B-GFP* mRNA showed a uniform distribution. One of two blastomeres injected with Vasa-MO (0.5 mM stock, lower panels) at 2-cell stage diminished the specific localization of *cyclinB* mRNA (arrows). See also supplementary material Fig. S6B for a quantitative analysis. Scale bars: 20 µm.

2006, 2010). Thus, it serves as an immune, negative control to complement the Vasa-pre-immune IgG control. The results show that pull-outs of Vasa and eIF4E contained a larger amount of RNAs compared with the Nanos2 or pre-immune IgG (supplementary material Fig. S5B), and RIP-qPCR results suggest that Vasa interacts with broad mRNA species at a similar level to eIF4E. This result suggests that Vasa functions by interacting with many different mRNAs for regulation of their translation, and not by a hierarchical interaction that indirectly affects translation more broadly (supplementary material Fig. S5C). From these results, we conclude that Vasa functions as a general translational regulator in these embryonic cells.

Vasa is specifically enriched in perinuclear granules during S phase and on the spindle during M phase (Yajima and Wessel, 2011b,c), and we hypothesized that Vasa might interact with a variety of mRNAs in these locations and function in efficient translation and/or distribution of mRNAs to the daughter cells in these large (relative to subsequent size of progeny; ∼100 µm diameter in first cell division and ∼10 µm in blastulae), rapidly dividing cells. We tested this hypothesis by visualizing various mRNA localizations by *in situ* hybridization (Fig. 5A; supplementary material Fig. S6A) and in live embryos (Fig. 5B; supplementary material Fig. S6B, Movie 1). Some mRNAs were discovered to be localized around the chromosomes during M phase and in perinuclear sites during S phase, very similar to the Vasa profile. This characteristic mRNA localization, however, was absent in Vasa-deficient embryos (Fig. 5A,B, Vasa-MO). Further, the human Histone 2B (H2B) mRNA, an exogenous reporter but known to be translated and localized in the nucleus of these embryonic cells (Yajima and Wessel, 2011b), showed no characteristic mRNA localization, yet did express GFP successfully in the nucleus (Fig. 5B; supplementary material Fig. S6B, Movie 2), suggesting that not all mRNAs interact equally with Vasa. Vasa in this embryo might thus interact with a pool of mRNAs by a selection mechanism that remains unclear. The selection for this Vasa-based broad mRNA interaction might be an increased translational efficiency, especially important in a large cell (∼100 µm diameter) that becomes rapidly dividing (lacking G phases), and is enhanced by translation locally using this mechanism during mitosis.

Vasa clusters mRNAs in an Importin-dependent manner during cell cycle progression

Using the Interactome database (Havugimana et al., 2012; Wan et al., 2013) (personal communications with Prof. Kathy Foltz at the University of California, San Diego; unpublished database), we identified Importin α2 (Kpna2) as a potential binding partner of Vasa. Importin α/β are known to form heterodimers and to target various proteins to the nuclear pore to shuttle them between the nucleus and the cytoplasm during S phase, as well as being required in formation of the spindle gradient during M phase (Goldfarb et al., 2004; Strom and Weis, 2001; Harel and Forbes, 2004). In the sea urchin embryo, Kpna2 did indeed localize similarly to Vasa in perinuclear regions during the S phase and on spindles during the M phase (Fig. 6A). Kpna2 immunoprecipitation (Kpna2-IP) pulled out Vasa (Fig. 6B) as well as Kpna2 itself, suggesting a physical interaction between Kpna2 and Vasa. Importazole (Soderholm et al., 2011), a specific functional inhibitor of Importin β, a partner of Kpna2, diminished the characteristic vasa mRNA and Vasa protein distribution, as well as other mRNA enrichment, both on the nuclear envelope and on the spindle (Fig. 6C, Importazole-Vasa IF; supplementary material Fig. S6A). Vasa-depletion, however, altered little of the Kpna2 localization either perinuclearly or on the spindle (Fig. 6A). Further, treatment of embryos with taxol, a microtubule stabilizer, resulted in excess Vasa protein and mRNA accumulation around the microtubules, implying that Vasa responded to microtubule arrays during the cell cycle (Fig. 6C, taxol-Vasa IF and -*vasa* ISH). These results suggest that Vasa depends on the cell ubiquitous Importin complex function for its positioning onto microtubules during somatic cell cycling.

The C-terminal proportion of Vasa (633-766aa of *S. purpuratus* Vasa) is responsible for both its specific localization and function in cell cycle progression (Gustafson et al., 2011; Yajima and Wessel,

Development (2015) 142, 1960-1970 doi:10.1242/dev.118448

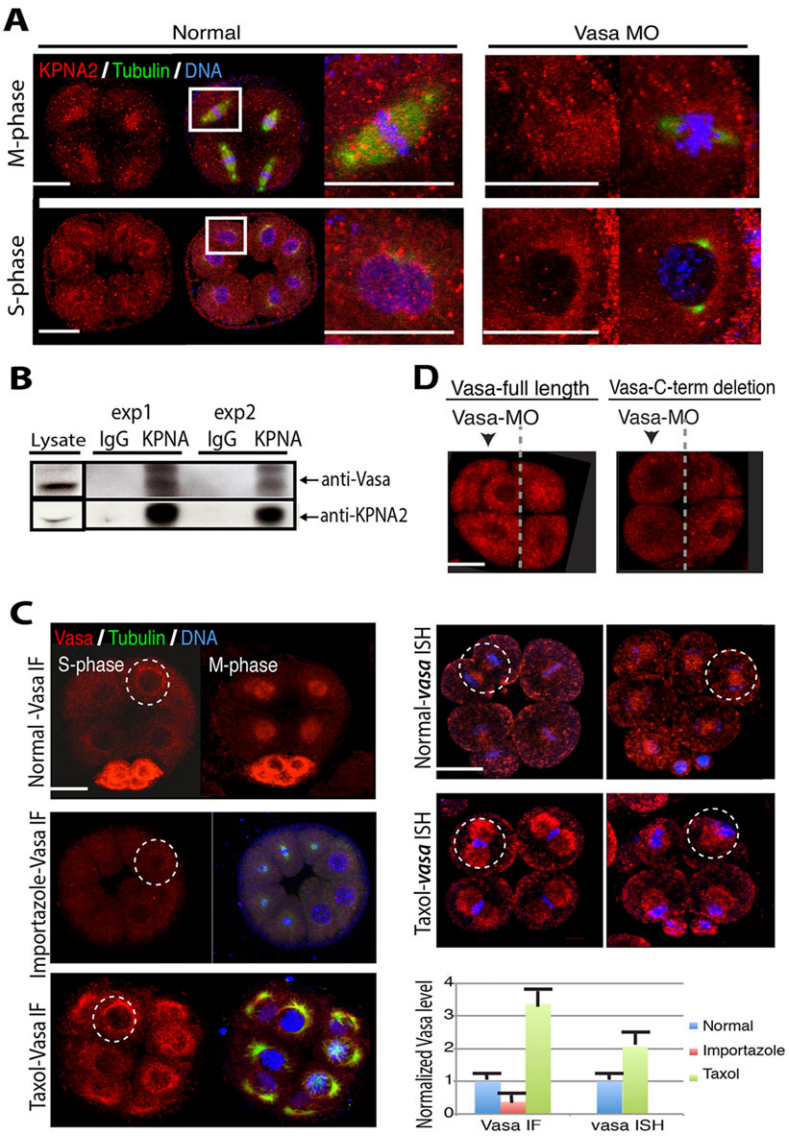

Fig. 6. Specific mRNA localization is regulated by Vasa and importins. Images were taken by confocal microscopy. (A) Immunofluorescence images of KPNA2 (red). KPNA2 was enriched in the spindle area during M phase, and at perinuclear areas and in the nucleus during S phase. Right panels in 'normal' are the higher magnification views of the squared regions in the middle panels. Vasa-MO panels show a representative cell of 4- to 8-cell-stage embryo injected with Vasa-MO (1 mM stock). Vasa-MO did not alter KPNA2 enrichment at perinuclear areas, yet reduced the signal around the spindle. Right panels show merged image of KPNA2, Tubulin and DNA signals. (B) Two examples of KPNA2-IP results. Vasa (doublet bands around 85 kDa; Gustafson et al., 2011) was immunoprecipitated with IgG (control) or anti-KPNA2 antibody. Each sample (2 µl) was loaded onto the gel and detected with anti-Vasa antibody by immunblotting. The same membrane was re-probed with anti-KPNA2 antibody (~65 kDa). Input (5 µl) was loaded for the 'lysate' lane. (C) Vasa protein localization was diminished by importazole treatment. Vasa protein (taxol-Vasa IF) and mRNA (taxol-*vasa* ISH) were over-enriched around the spindle by taxol. The same setting was used to capture each image by confocal microscopy. A graph indicates the signal intensity of Vasa (red) measured in the regions denoted by white dashed circles. Each signal was calculated by ImageJ for five individual embryos per sample. The averaged value of each sample was normalized to that of normal embryos. (D) Live imaging of *cyclinB* mRNA labelled by Alexa 546-UTP. Labelled mRNA was injected with full-length or C-terminal-depleted *Vasa*-mRNA into the fertilized eggs, and then Vasa-MO was injected into the left half of 2-cell-stage embryos. A dashed line demarcates Vasa-MO-injected blastomeres (left) and intact blastomere (right). A perinuclear localization of *cyclinB* was rescued by full-length deletion (Vasa-full length) but not by C-terminus deletion of Vasa (Vasa-C-term deletion). Scale bars: 20 µm.

2011b) and is important for its translational activity in *Drosophila* (617aa of *D. melanogaster* Vasa) (Liu et al., 2009). We found that Vasa lacking the C-terminus failed to recover the mRNA clustering activity in Vasa-deficient embryos (Fig. 6D, Vasa-C-term deletion), whereas a full-length Vasa successfully rescued a granular distribution of mRNAs (Fig. 6D, Vasa-full length), suggesting the Vasa C-terminus is important for multiple functions of Vasa, including its mRNA clustering activities. Currently, we do not know the mechanisms of mRNA clustering, but this phenotype of the molecule appears to be an important metric for its functionality in the germline and in somatic cells.

DISCUSSION

Vasa expression has long been used as a germline marker. It is, however, apparent, when looking outside some of the most intensively studied organisms, such as flies, worms, mice and fish, that many animals stray from this original paradigm. Indeed, the more broadly investigators examine non-traditional model organisms, the more diverse the original 'germline factors' become in cell expression and function. Further, these factors also appear to have multiple functions within a cell. For Vasa specifically, this includes recently documented functions recruited to the mitotic spindle both in the germ line and in somatic lineages (Rouhana et al., 2010; Lerit and Gavis, 2011; Pek and Kai, 2011; Yajima and Wessel, 2011b,c; Wagner et al., 2012).

We previously hypothesized that an ancient character of Vasa-like DEAD-box protein might have been in regulation of a rapid cell cycling in a large cell (Yajima and Wessel, 2011b,c), and the results in the present study provide mechanistic insight into this process. Even though Vasa has long been known and observed in many different organisms, it is rare to see Vasa expressed as dynamically as in sea urchins. Perhaps this reflects a vast regulative and regenerative capability of this embryo and adult. In addition, Vasa-expressing cells are more highly proliferative cells relative to their neighbours or sibling Vasa-null cells. The exception to this rule is the germ line (small-micromere lineage in the sea urchin), which enriches Vasa the most but has the slowest cell cycle in the embryo (Pehrson and Cohen, 1986; Tanaka and Dan, 1990). In the small micromeres, however, the cell-cycle suppressor Nanos is also expressed, probably as a dominant game changer in cell cycling activity (Juliano et al., 2010). Cell cycling in the early sea urchin embryo is rapid (20 min for M phase, 20 min for S phase and no G phase) and the cells are large, beginning at ~100 µm in diameter, compared with cells in the

Development (2015) 142, 1960-1970 doi:10.1242/dev.118448

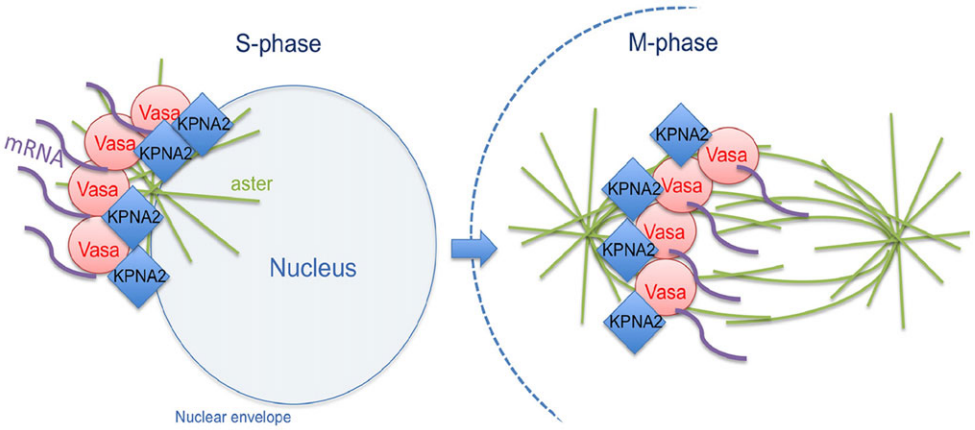

Fig. 7. A hypothetical model of Vasa function in the somatic multipotent cells. A model of Vasa function in mRNA shuttling during rapid embryonic cell cycle progression. A protein complex of KPNA2 and Vasa shuttles various mRNAs necessary for embryogenesis between cytoplasm and spindle during rapid cell cycle progression of the embryo.

differentiated tissues of the sea urchin. In those cells, Vasa might function in enhancing mRNA positioning for proper distribution and efficient translation, not just during S phase but also during M phase, to enhance rapid cell cycle progression (Blower et al., 2007) (Fig. 7). The conundrum for the field, however, is that Vasa appears to be essential in cells that express Vasa. As not all cells have Vasa, and yet function perfectly well, it is not clear what must be different in Vasa-expressing cells.

Here, we demonstrated that Vasa is essential for several developmental events, including reprogramming of cells in the embryos, wound healing of larval tissues and translational activity. The detailed mechanism of damage recovery followed by regeneration in this organism is still poorly understood, yet echinoderm regeneration appears to share many features with e.g. planarian regeneration. These animals are capable of regenerating most of their tissues, including gonads, and are regulated not by lineage-restricted unipotent stem cells but rather by pluripotent stem cells (Guo et al., 2006; Wagner et al., 2011). In the planarian, many germline-related genes, such as *nanos*, *spoltud-1*, *smedwi-1*, *smedwi-2*, *bruno-like* and *pumilio*, have been demonstrated to be involved in the regeneration process and the regenerative process dependent upon pluripotent stem cells, the neoblasts (Wang et al., 2007; Solana et al., 2009; Fernandez-Taboada et al., 2010; Scimone et al., 2010; Aboobaker, 2011). The expression of a Vasa-related DEAD-box protein, PL10, was reported to reside in the neoblasts (Shibata et al., 1999). More recently, genes encoding Vasa have been reported to be required for regeneration (Rouhana et al., 2010) or for proliferation of neoblast descendants (Wagner et al., 2012), thus implying Vasa's functionality in regeneration along with other germline-related genes expressed in neoblasts. The results herein then might indicate the mechanism of how the neoblasts make use of Vasa for its essential roles in regeneration, and how broadly Vasa functions in regenerative activities.

In summary, we conclude that Vasa has retained an ancient role as a multipotent cell regulator more effectively in sea urchins, presumably controlling mRNA translocation and translation of regulators for rapid and efficient embryogenesis. Vasa expression in the non-germ-cell lineage has been reported also in embryos of other organisms, such as of annelids and chaetognaths (Oyama and Shimizu, 2007; Carré et al., 2002), supporting this hypothesis. Additionally, a recent report involving spider development (Schwager et al., 2014) further supports the hypothesis of the role of Vasa in mitotic cell cycle progression in embryonic multipotent cells. We cannot rule out additional Vasa function in regulating piRNA production, as recently reported in flies (Xiol et al., 2014). The sea urchin embryo does have a large population of both miRNAs and piRNAs (Song et al., 2012), yet the phenotypes of Piwi, Drosha or Dicer knockdowns do not show a similar phenotype as the Vasa knockdown demonstrated in this report (Song et al., 2012; Yajima et al., 2014). Therefore, the somatic function of Vasa seen in the sea urchin might be independent of the piRNA (or miRNA) pathways, at least for the phenotypes seen herein. This is the first report that gives a mechanistic insight into Vasa function in somatic cell lineages, which is probably a conserved and fundamental function of this enigmatic molecule among organisms.

MATERIALS AND METHODS

Strongylocentrotus purpuratus were collected in Long Beach, California, USA (Point Loma Marine Invertebrate Lab), and *Lytechinus variegatus* were from Florida, USA (KP Aquatics). Handling, culture and gamete procurement followed standard protocol (Ettensohn et al., 2004). Larvae were cultured and fed on *Chaetoceros gracilis* (UTEX), as previously described (Yajima, 2007). Immunolabelling was conducted as previously described (Yajima and Kiyomoto, 2006; Voronina et al., 2008). Anti-SpVasa (Voronina et al., 2008), anti-KPNA2 antibody (Novus Biologicals, NB100-79807; 1.0 mg/ml stock) and anti-BrdU monoclonal antibody (Sigma, #B2531) were used at final concentrations of 1:300, 1:500 and 1:200, respectively. The secondary antibodies conjugated to Cy3, Alexa 488 or Alexa 594 (all by Invitrogen) were used at final concentrations of 1:250, 1:500 and 1:500, respectively. Embryo manipulations and imaging were performed as described previously (Yajima, 2007; Yajima and Wessel, 2011a), and Vasa-GFP protocols were previously described by Gustafson et al. (2011) and Yajima and Wessel (2011b, 2012). This protocol was confirmed to replicate the endogenous Vasa expression and to rescue the cell-cycle defects in Vasa-MO-injected embryos (Gustafson et al., 2011). Ne-GFP and H2B (Histone2B)-EGFP were gifts from Dr Yasunori Sasakura at Tsukuba University, Japan, and from Dr Sean Megason at Harvard University, USA (GenBankFiles \p005_pCS-H2B-EGFP.gb), respectively. The specificity and controls for the Sp-vasa morpholino (Vasa-MO) was previously documented (Gustafson et al., 2011; Yajima and Wessel, 2011b). Labelling of mRNA and injection were performed as described (Gagnon and Mowry, 2011), using Alexa 546-UTP in the SP6 mMessage mMachine (Ambion) protocol. Quantitative RT-PCR was performed as described (Juliano et al., 2006), using PCR primers listed in the supplementary material Table S1. The protocol for *in situ* RNA hybridization was as described (Arenas-Mena et al., 2000; Yajima et al., 2013). Protein synthesis was determined using ^{35}S-methionine (200 µCi) incorporation and roscovitine was used at a final concentration of 0.1 µM. The immunoprecipitation protocol (IP) is documented in the supplementary materials methods. Antibodies used for the IP procedure were affinity-purified anti-Vasa (Voronina et al., 2008), anti-KPNA2 antibody (Novus Biologicals, NB100-79807; 1.0 mg/ml stock) and YP30 (Wessel et al., 2000). Inhibitors used in embryo treatment included 100 µM importazole (Sigma, SML0341) or 100 µM taxol

(Sigma, Paclitaxel-T7402). Please see the supplementary materials methods for a full description of materials and methods.

Acknowledgements
We thank Professor Kathy Foltz at UCSB (kathy.foltz@lifesci.ucsb.edu) for sharing a list of Vasa-interactors from their Interactome database and members of PRIMO for critical discussions and support.

Competing interests
The authors declare no competing or financial interests.

Author contributions
M.Y. was responsible for concepts, experimental design and undertaking, data analysis, manuscript construction and editing; G.M.W. was responsible for conceptualization, experimental design, manuscript construction and editing.

Funding
This work was supported by the National Institutes of Health [2R01HD028152] and the National Science Foundation [IOS-1120972] grants to G.M.W.; and by the American Heart Association Scientist Development Grant [14SDG18350021] and a Human Frontier Science Program long-term fellowship to M.Y. Deposited in PMC for release after 12 months.

Supplementary material
Supplementary material available online at
http://dev.biologists.org/lookup/suppl/doi:10.1242/dev.118448/-/DC1

References

Aboobaker, A. A. (2011). Planarian stem cells: a simple paradigm for regeneration. *Trends Cell Biol.* **21**, 304-311.
Arenas-Mena, C., Cameron, A. R. and Davidson, E. H. (2000). Spatial expression of Hox cluster genes in the ontogeny of a sea urchin. *Development* **127**, 4631-4643.
Blower, M. D., Feric, E., Weis, K. and Heald, R. (2007). Genome-wide analysis demonstrates conserved localization of messenger RNAs to mitotic microtubules. *J. Cell Biol.* **179**, 1365-1373.
Bosch, I., Rivkin, R. B. and Alexander, S. P. (1989). Asexual reproduction by oceanic planktotrophic echinoderm larvae. *Nature* **337**, 169-170.
Cameron, R. A., Hough-Evans, B. R., Britten, R. J. and Davidson, E. H. (1987). Lineage and fate of each blastomere of the eight-cell sea urchin embryo. *Genes Dev.* **1**, 75-85.
Cameron, R. A., Fraser, S. E., Britten, R. J. and Davidson, E. H. (1991). Macromere cell fates during sea urchin development. *Development* **113**, 1085-1092.
Carré, D., Djediat, C. and Sardet, C. (2002). Formation of a large Vasa-positive germ granule and its inheritance by germ cells in the enigmatic Chaetognaths. *Development* **129**, 661-670.
Dubois, P. and Ameye, L. (2001). Regeneration of spines and pedicellariae in echinoderms: a review. *Microsc. Res. Tech.* **55**, 427-437.
Eaves, A. A. and Palmer, A. R. (2003). Reproduction: widespread cloning in echinoderm larvae. *Nature* **425**, 146.
Emson, R. H. and Wilkie, I. C. (1980). Fission and autotomy in echinoderms. *Oceanogr. Mar. Biol. Annu. Rev.* **18**, 155-250.
Ettensohn, C. A., Wessel, G. M. and Wray, G., ed. (2004). *Development of Sea Urchins, Ascidians and Other Non-Vertebrate Deuterostomes: An Experimental Analysis*. London, UK: Academic Press.
Fernandez-Taboada, E., Moritz, S., Zeuschner, D., Stehling, M., Scholer, H. R., Salo, E. and Gentile, L. (2010). Smed-SmB, a member of the LSm protein superfamily, is essential for chromatoid body organization and planarian stem cell proliferation. *Development* **137**, 1055-1065.
Gagnon, J. A. and Mowry, K. L. (2011). Visualization of mRNA localization in Xenopus oocytes. *Methods Mol. Biol.* **714**, 71-82.
Goldfarb, D. S., Corbett, A. H., Mason, D. A., Harreman, M. T. and Adam, S. A. (2004). Importin alpha: a multipurpose nuclear-transport receptor. *Trends Cell Biol.* **14**, 505-514.
Goss, R. J.ed. (1969). *Principles of Regeneration*. London: Academic Press.
Guo, T., Peters, A. H. F. M. and Newmark, P. A. (2006). A bruno-like gene is required for stem cell maintenance in planarians. *Dev. Cell* **11**, 159-169.
Gustafson, E. A. and Wessel, G. M. (2010a). DEAD-box helicases: posttranslational regulation and function. *Biochem. Biophys. Res. Commun.* **395**, 1-6.
Gustafson, E. A. and Wessel, G. M. (2010b). Vasa genes: emerging roles in the germ line and in multipotent cells. *BioEssays* **32**, 626-637.
Gustafson, E. A., Yajima, M., Juliano, C. E. and Wessel, G. M. (2011). Post-translational regulation by gustavus contributes to selective Vasa protein accumulation in multipotent cells during embryogenesis. *Dev. Biol.* **349**, 440-450.
Harel, A. and Forbes, D. J. (2004). Importin beta: conducting a much larger cellular symphony. *Mol. Cell* **16**, 319-330.
Havugimana, P. C., Hart, G. T., Nepusz, T., Yang, H., Turinsky, A. L., Li, Z., Wang, P. I., Boutz, D. R., Fong, V., Phanse, S. et al. (2012). A census of human soluble protein complexes. *Cell* **150**, 1068-1081.
Hay, B., Jan, L. Y. and Jan, Y. N. (1988). A protein component of *Drosophila* polar granules is encoded by *vasa* and has extensive sequence similarity to ATP-dependent helicases. *Cell* **55**, 577-587.
Horstadius, S. (1950). The mechanics of sea urchin development. *Annee Biol.* **26**, 381-398.
Horstadius, S. (1973). *Experimental Embryology of Echinoderms*. Oxford: Clarendon Press.
Janic, A., Mendizabal, L., Llamazares, S., Rossell, D. and Gonzalez, C. (2010). Ectopic expression of germline genes drives malignant brain tumor growth in Drosophila. *Science* **330**, 1824-1827.
Juliano, C. E. and Wessel, G. M. (2009). An evolutionary transition of vasa regulation in echinoderms. *Evol. Dev.* **11**, 560-573.
Juliano, C. and Wessel, G. (2010). Versatile germline genes. *Science* **329**, 640-641.
Juliano, C. E., Voronina, E., Stack, C., Aldrich, M., Cameron, A. R. and Wessel, G. M. (2006). Germ line determinants are not localized early in sea urchin development, but do accumulate in the small micromere lineage. *Dev. Biol.* **300**, 406-415.
Juliano, C. E., Yajima, M. and Wessel, G. M. (2010). Nanos functions to maintain the fate of the small micromere lineage in the sea urchin embryo. *Dev. Biol.* **337**, 220-232.
Lasko, P. (2013). The DEAD-box helicase Vasa: evidence for a multiplicity of functions in RNA processes and developmental biology. *Biochem. Biophys. Acta* **1829**, 810-816.
Lasko, P. F. and Ashburner, M. (1988). The product of the Drosophila gene vasa is very similar to eukaryotic initiation factor-4A. *Nature* **335**, 611-617.
Lasko, P. F. and Ashburner, M. (1990). Posterior localization of vasa protein correlates with, but is not sufficient for, pole cell development. *Genes Dev.* **4**, 905-921.
Lerit, D. A. and Gavis, E. R. (2011). Transport of germ plasm on astral microtubules directs germ cell development in Drosophila. *Curr. Biol.* **21**, 439-448.
Liu, N., Han, H. and Lasko, P. (2009). Vasa promotes Drosophila germline stem cell differentiation by activating mei-P26 translation by directly interacting with a (U)-rich motif in its 3′ UTR. *Genes Dev.* **23**, 2742-2752.
Mashanov, V. and García-Arrarás, J. E. (2011). Gut regeneration in holothurians: a snapshot of recent developments. *Biol. Bull.* **221**, 93-109.
Materna, S. C., Swartz, S. Z. and Smith, J. (2013). Notch and Nodal control forkhead factor expression in the specification of multipotent progenitors in sea urchin. *Development* **140**, 1796-1806.
Oyama, A. and Shimizu, T. (2007). Transient occurrence of vasa-expressing cells in nongenital segments during embryonic development in the oligochaete annelid Tubifex tubifex. *Dev. Genes Evol.* **217**, 675-690.
Paz-Gómez, D., Villanueva-Chimal, E. and Navarro, R. E. (2014). The DEAD box RNA helicase VBH-1 is a new player in the stress response in C. elegans. *PLoS ONE* **9**, e97924.
Pek, J. W. and Kai, T. (2011). A role for vasa in regulating mitotic chromosome condensation in Drosophila. *Curr. Biol.* **21**, 39-44.
Pehrson, J. R. and Cohen, L. H. (1986). The fate of the small micromeres in sea urchin development. *Dev. Biol.* **113**, 522-526.
Ransick, A. and Davidson, E. H. (1993). A complete second gut induced by transplanted micromeres in the sea urchin embryo. *Science* **259**, 1134-1138.
Raz, E. (2000). The function and regulation of vasa-like genes in germ-cell development. *Genome Biol.* **1**, reviews1017-reviews1017.6.
Rebscher, N., Zelada-González, F., Banisch, T. U., Raible, F. and Arendt, D. (2007). Vasa unveils a common origin of germ cells and of somatic stem cells from the posterior growth zone in the polychaete Platynereis dumerilii. *Dev. Biol.* **306**, 599-611.
Rouhana, L., Shibata, N., Nishimura, O. and Agata, K. (2010). Different requirements for conserved post-transcriptional regulators in planarian regeneration and stem cell maintenance. *Dev. Biol.* **341**, 429-443.
Saga, Y. (2010). Function of Nanos2 in the male germ cell lineage in mice. *Cell. Mol. Life Sci.* **67**, 3815-3822.
Schwager, E. E., Meng, Y. and Extavour, C. G. (2014). Vasa and piwi are required for mitotic integrity in early embryogenesis in the spider Parasteatoda tepidariorum. *Dev. Biol.* (in press).
Scimone, M. L., Meisel, J. and Reddien, P. W. (2010). The Mi-2-like Smed-CHD4 gene is required for stem cell differentiation in the planarian Schmidtea mediterranea. *Development* **137**, 1231-1241.
Shibata, N., Umesono, Y., Orii, H., Sakurai, T., Watanabe, K. and Agata, K. (1999). Expression of vasa (vas)-related genes in germline cells and totipotent somatic stem cells of planarians. *Dev. Biol.* **206**, 73-87.
Soderholm, J. F., Bird, S. L., Kalab, P., Sampathkumar, Y., Hasegawa, K., Uehara-Bingen, M., Weis, K. and Heald, R. (2011). Importazole, a small molecule inhibitor of the transport receptor importin-β. *ACS Chem. Biol.* **6**, 700-708.
Solana, J., Lasko, P. and Romero, R. (2009). Spoltud-1 is a chromatoid body component required for planarian long-term stem cell self-renewal. *Dev. Biol.* **328**, 410-421.

Song, J. L., Stoeckius, M., Maaskola, J., Friedländer, M., Stepicheva, N., Juliano, C., Lebedeva, S., Thompson, W., Rajewsky, N. and Wessel, G. M. (2012). Select microRNAs are essential for early development in the sea urchin. *Dev. Biol.* **362**, 104-113.

Ström, A.-C. and Weis, K. (2001). Importin-beta-like nuclear transport receptors. *Genome Biol.* **2**, reviews3008-reviews3008.9.

Tanaka, S. and Dan, K. (1990). Study of the lineage and cell cycle of small micromeres in embryos of the sea urchin, *Hemicentrotus pulcherrimus*. *Dev. Growth Differ.* **32**, 145-156.

Topisirovic, I., Svitkin, Y. V., Sonenberg, N. and Shatkin, A. J. (2011). Cap and cap-binding proteins in the control of gene expression. *Wiley Interdiscip. Rev. RNA* **2**, 277-298.

Vaughn, D. and Strathmann, R. R. (2008). Predators induce cloning in echinoderm larvae. *Science* **319**, 1503.

Voronina, E., Lopez, M., Juliano, C. E., Gustafson, E., Song, J. L., Extavour, C., George, S., Oliveri, P., McClay, D. and Wessel, G. (2008). Vasa protein expression is restricted to the small micromeres of the sea urchin, but is inducible in other lineages early in development. *Dev. Biol.* **314**, 276-286.

Wagner, D. E., Wang, I. E. and Reddien, P. W. (2011). Clonogenic neoblasts are pluripotent adult stem cells that underlie planarian regeneration. *Science* **332**, 811-816.

Wagner, D. E., Ho, J. J. and Reddien, P. W. (2012). Genetic regulators of a pluripotent adult stem cell system in planarians identified by RNAi and clonal analysis. *Cell Stem Cell* **10**, 299-311.

Wan, C., Liu, J., Fong, V., Lugowski, A., Stoilova, S., Bethune-Waddell, D., Borgeson, B., Havugimana, P. C., Marcotte, E. M. and Emili, A. (2013). ComplexQuant: high-throughput computational pipeline for the global quantitative analysis of endogenous soluble protein complexes using high resolution protein HPLC and precision label-free LC/MS/MS. *J. Proteomics* **81**, 102-111.

Wang, Y., Zayas, R. M., Guo, T. and Newmark, P. A. (2007). nanos function is essential for development and regeneration of planarian germ cells. *Proc. Natl. Acad. Sci. USA* **104**, 5901-5906.

Wessel, G. M., Zaydfudim, V., Hsu, Y.-t. J., Laidlaw, M. and Brooks, J. M. (2000). Direct molecular interaction of a conserved yolk granule protein in sea urchins. *Dev. Growth Differ.* **42**, 507-517.

Xiol, J., Spinelli, P., Laussmann, M. A., Homolka, D., Yang, Z., Cora, E., Couté, Y., Conn, S., Kadlec, J., Sachidanandam, R. et al. (2014). RNA clamping by Vasa assembles a piRNA amplifier complex on transposon transcripts. *Cell* **157**, 1698-1711.

Yajima, M. (2007). A switch in the cellular basis of skeletogenesis in late-stage sea urchin larvae. *Dev. Biol.* **307**, 272-281.

Yajima, M. and Kiyomoto, M. (2006). Study of larval and adult skeletogenic cells in developing sea urchin larvae. *Biol. Bull.* **211**, 183-192.

Yajima, M. and Wessel, G. M. (2011a). Small micromeres contribute to the germline in the sea urchin. *Development* **138**, 237-243.

Yajima, M. and Wessel, G. M. (2011b). The DEAD-box RNA helicase Vasa functions in embryonic mitotic progression in the sea urchin. *Development* **138**, 2217-2222.

Yajima, M. and Wessel, G. M. (2011c). The multiple hats of Vasa: its functions in the germline and in cell cycle progression. *Mol. Reprod. Dev.* **78**, 861-867.

Yajima, M. and Wessel, G. M. (2012). Autonomy in specification of primordial germ cells and their passive translocation in the sea urchin. *Development* **139**, 3786-3794.

Yajima, M., Suglia, E., Gustafson, E. A. and Wessel, G. M. (2013). Meiotic gene expression initiates during larval development in the sea urchin. *Dev. Dyn.* **242**, 155-163.

Yajima, M., Gustafson, E. A., Song, J. L. and Wessel, G. M. (2014). Piwi regulates Vasa accumulation during embryogenesis in the sea urchin. *Dev. Dyn.* **243**, 451-458.

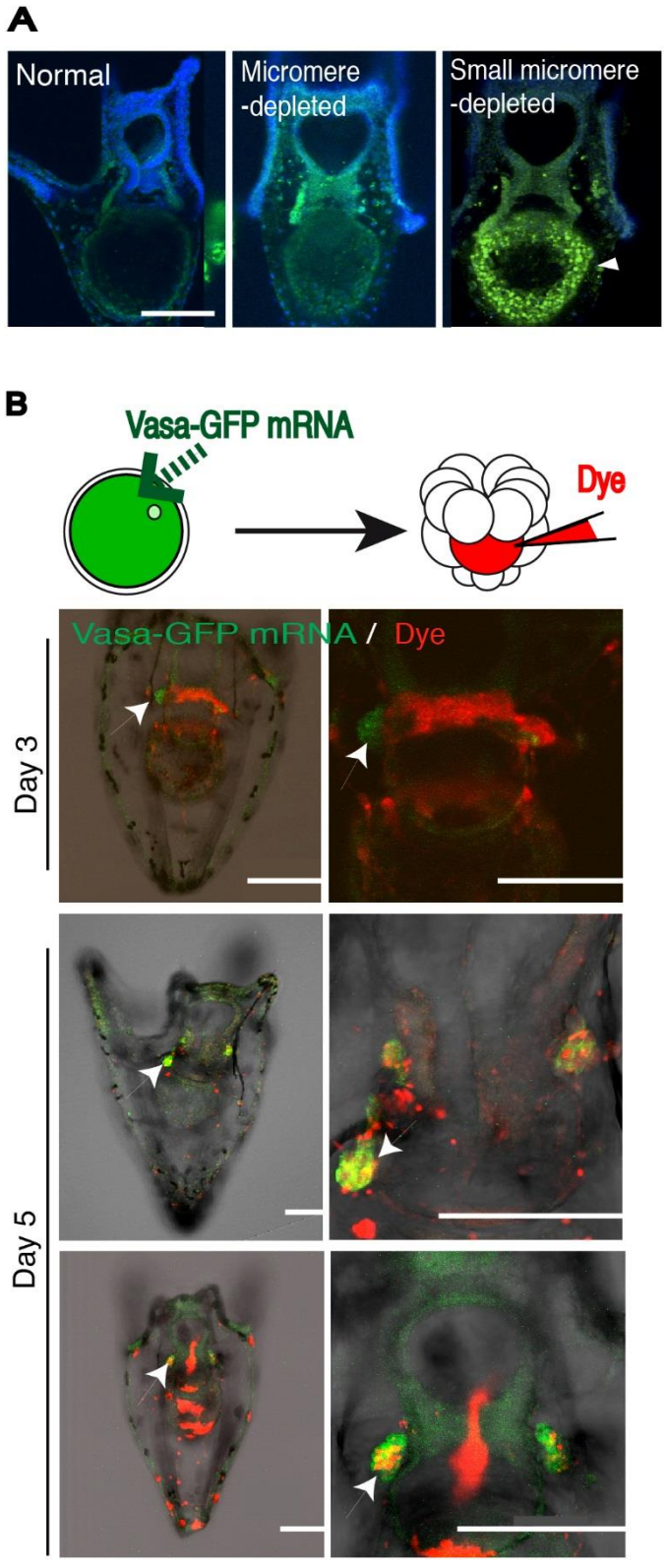

Figure S1, related to Figure 1. A transition from symmetric to asymmetric expression of Vasa in coelomic pouches. **A,** Vasa-positive micromeres /small micromeres were surgically depleted at 16-32 cell stages. Vasa-positive cells were not found during early development (Yajima and Wessel, 2011a), yet reappeared in the coelomic pouches of the Day 5 feeding *L. variegates* larvae, suggesting an involvement of another

lineage in this Vasa expression. Vasa (green), Hoechst (blue). An arrowhead in the stomach indicates background fluorescence derived from algae. Z-stack projection images, focusing only on the surface of coelomic pouches, were taken by confocal microscopy. **B,** To test if macromere descendants are involved, Vasa-GFP mRNA was injected into a fertilized egg and a single macromere was labelled with the fluorescent dye. Vasa-positive cells (green) were restricted into the small micromere lineage until early larvae (Day 3, arrows) yet the labelled macromere descendants (red) appear to become positive with Vasa-GFP signal in late larvae (Day 5, arrows), demonstrating a potential contribution of macromere (non-germ line) lineage to the Vasa-positive population in an expanding coelomic pouch at late larval stages. Scale bars = 50 μm. Images were taken by confocal microscopy and merged over to the bright field.

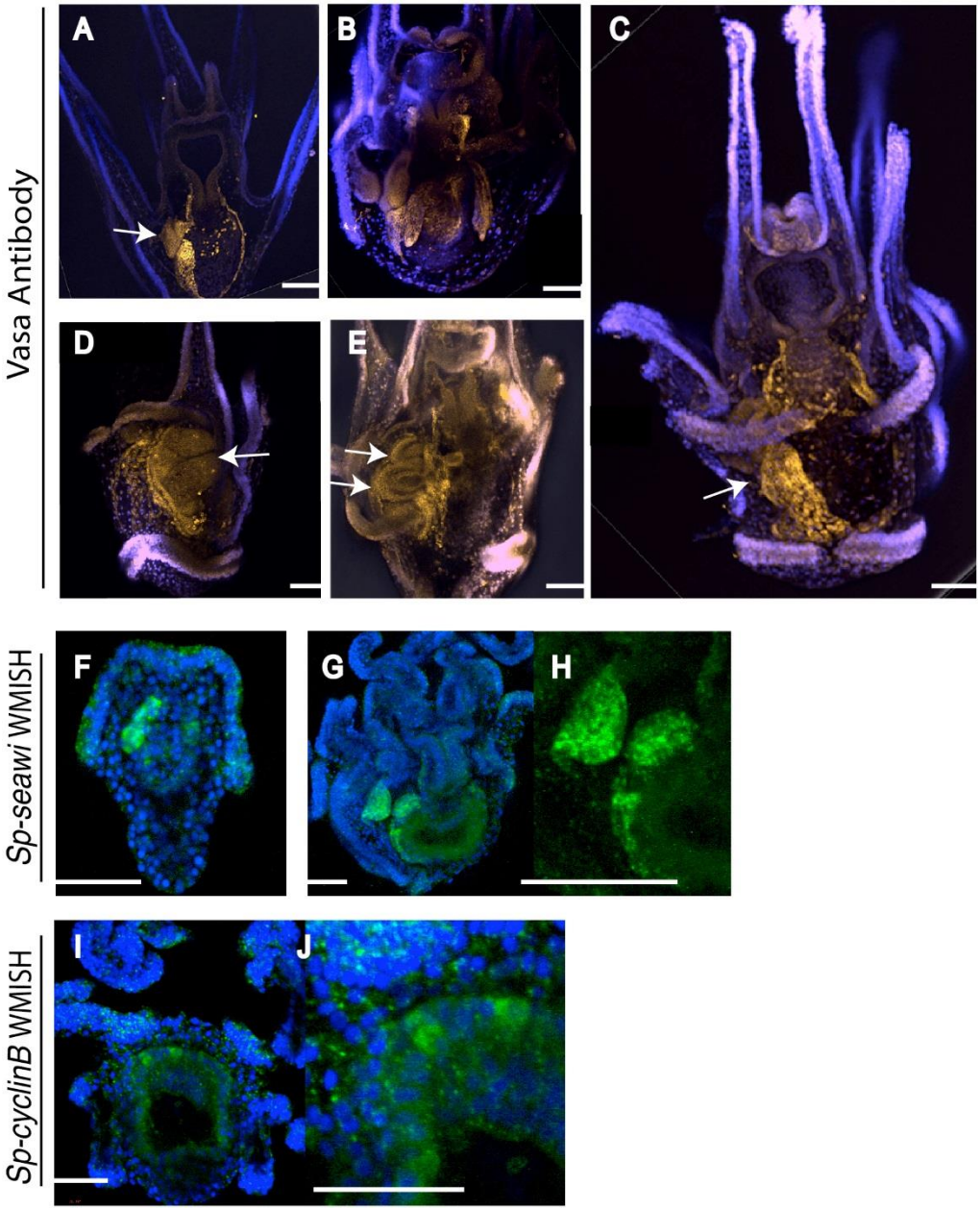

Figure S2, related to Figure 1. Vasa expression during late larval stage. Images were taken by confocal microscopy. **A-E,** High levels of Vasa accumulation continued during development in the entire adult rudiment including somatic adult structures, together with a low signal in the mouth and intestine of the larva. Late larvae from 6-armed pluteus (A), 8-armed pluteus (B and C), and metamorphic larvae (D and E) were immunolabelled with Vasa-antibody (yellow, arrows) and counterstained with Hoechst (blue). From the morphology and the location of labeling, many of the Vasa-positive cells are apparently progenitors of adult structures such as spines, tests, water vascular and neuronal system and tube feet. The levels of Vasa signal were dynamic and its decrease was seen upon differentiation in the adult rudiment by the end of the larval stage and at the onset of metamorphosis. **F-H,** another germ line marker *seawi* mRNA (green) was specifically localized in the coelomic pouch (F) and the adult rudiment (G and H). H is a magnified view of the adult rudiment in G. **I and J,** the positive cell cycle regulator *cyclinB* mRNA (green) was localized in the adult rudiment of the late larvae. J is a magnified view of the adult rudiment in I. Scale bars = 50 μm.

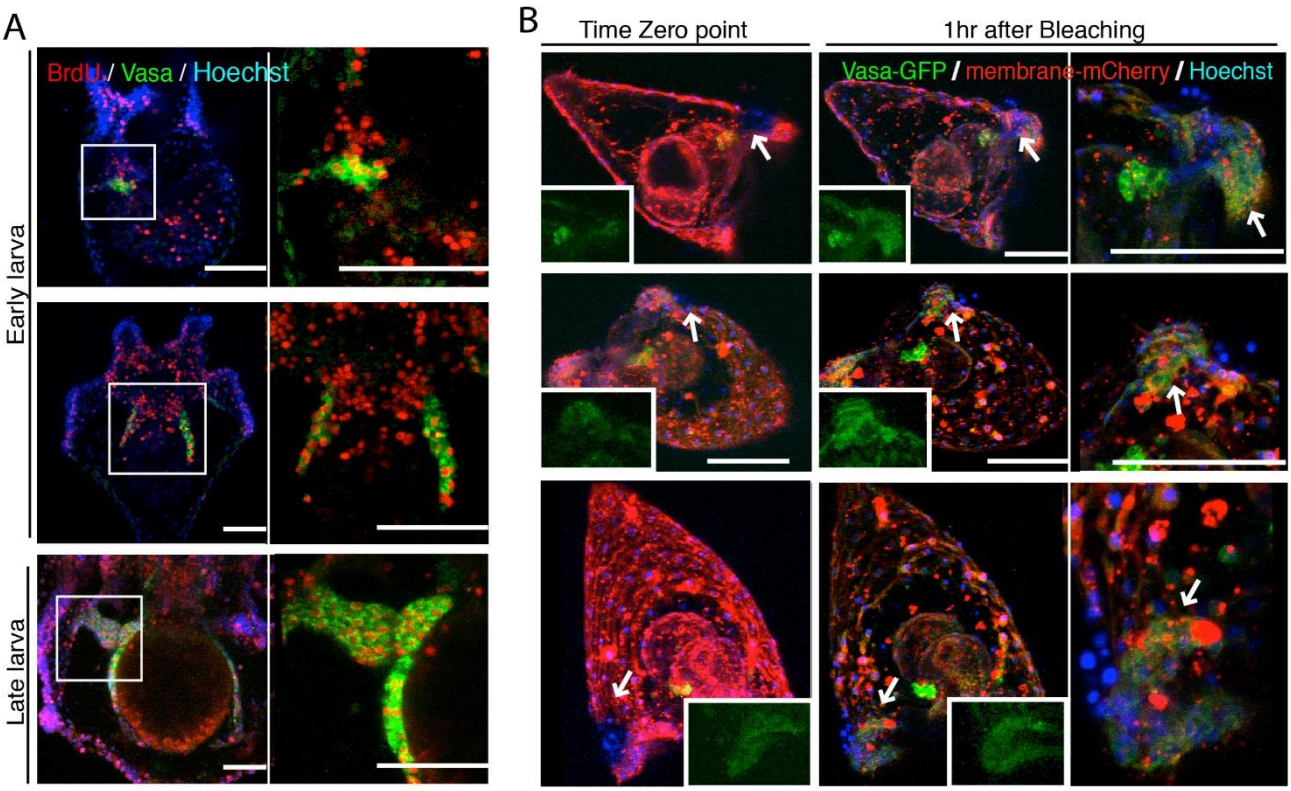

Figure S3, related to Figure 2. Vasa-positive cells in the adult rudiment are highly proliferative and the ectopic Vasa expression was induced in response to the damage. **A,** Upper two panels are 1-week old larvae and the bottom panel is a two-weeks old larva with starting adult rudiment formation. Vasa (green)-positive cells are also co-labeled with BrdU (red) within 1hr of BrdU-treatment, and counterstained with Hoechst (blue). White squares indicate the enlarged region on the right of each panel. Images were taken by confocal microscopy. **B,** Three examples of Day5 larvae injected or labeled with Vasa-GFP (green), membrane-mCherry (Red) and Hoechst (Blue) are shown. A small region of each larval body was damaged by laser-energy (arrows in Left panels) and the ectopic expression of Vasa-GFP around the damaged area was observed after 1hr of the ablation (arrows in Middle and Right panels). Membrane-mCherry that is consistently expressed independent of damage was used to normalize the signal level of Vasa-GFP. Relative signal intensity of GFP to mCherry of the same region was calculated before or after bleaching by *Image J*. Insets are a single channel for GFP. Each right panel is an enlarged view of each middle panel. Middle and Right panels are constructed from a subset of Z-stack images to focus only in the region of interest. Scale bars = 50 μm.

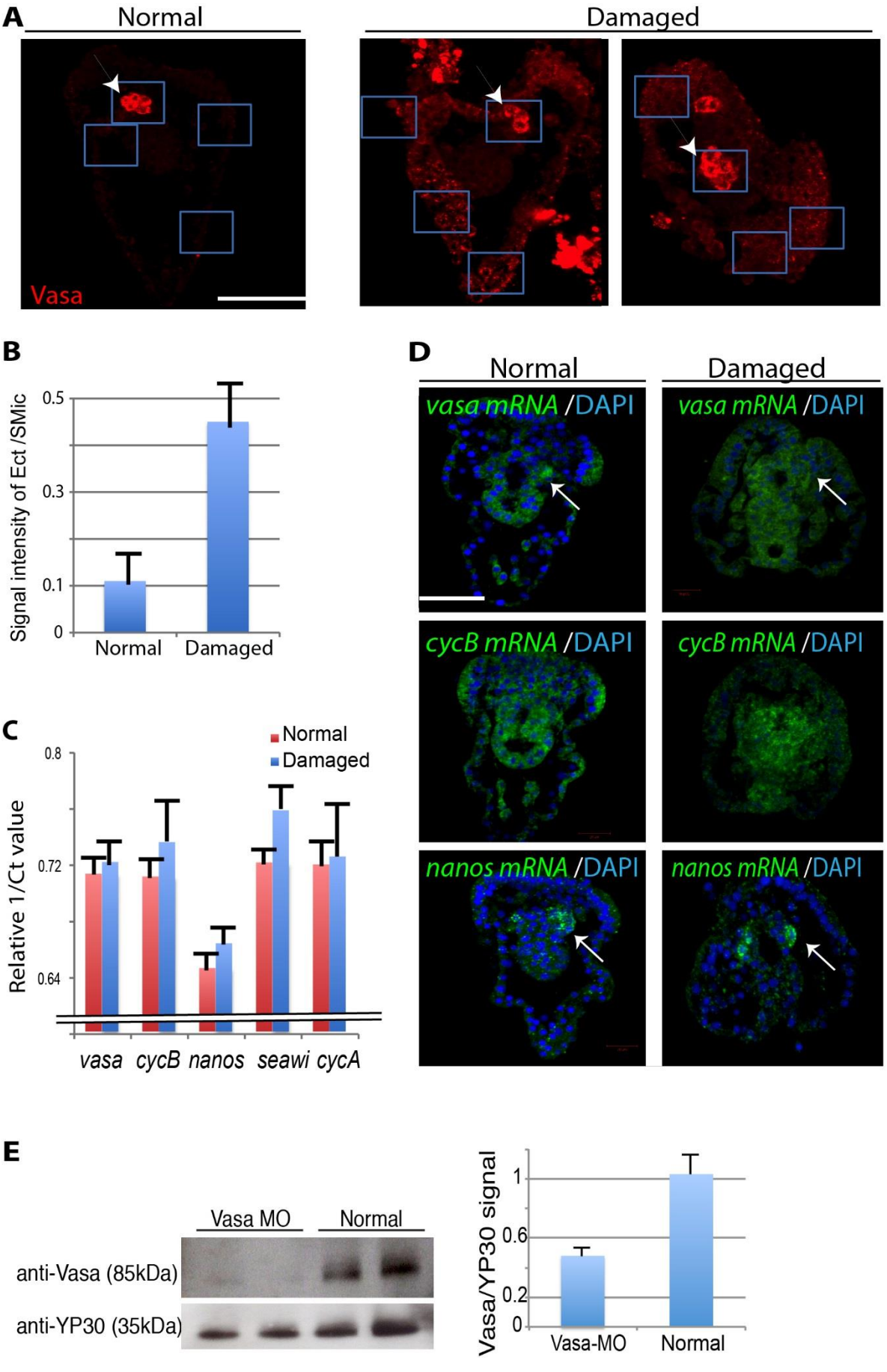

Figure S4, related to Figure 3. The post-transcriptional regulation of Vasa is essential for developmental re-programming. Images were taken by confocal microscopy. **A and B,** A half body of Day3 larvae were

damaged by a glass needle and that induced ectopic Vasa over-expression nearly in the entire larval body (A). The squares are the regions where the ectopic Vasa signal in the ectoderm was quantified by *image J* and compared to the signal in the small micromere descendants (arrows). The small micromeres in this experiment were left intact, and thus Vasa signal in this lineage is unaffected by the damage that serves as a control. Two of the representative images of damaged larvae are shown. In those larvae, over 4 times increase of the Vasa signal was found in the ectodermal tissues within 1hr after damage (B) compared to the non-damaged larvae. Error bars indicate SD of averaged signal level obtained from five individual larvae. **C,** Damaged larvae demonstrated little increase in the transcripts encoding *vasa, cyclinB, nanos2, seawi, cyclinA*. Error bars indicate SD of three independent experiments. **D,** Damaged larvae showed expanded expression of *vasa* and *cyclinB* yet had little effect on *nanos* mRNA localization. Arrows indicate the small micromere descendants. Scale bars = 50 μm. **E,** The immunoblot analysis of Vasa-MO knockdown. Vasa is maternally loaded yet the zygotic Vasa appears to be reduced in Vasa-MO injected embryos (Vasa-MO) compare to the uninjected embryos (Normal). A right graph indicates the signal intensity of each band normalized by YP30 (Yolk protein 30, that is consistently present independent of Vasa function) and quantified by *Image J*. Error bars indicate SD of three independent experiments.

A

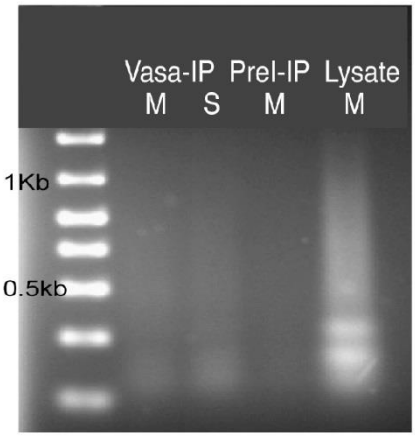

B

SAMPLE	Amount of mRNA IP-ed	% of Vasa-interacting mRNA amount in the lysate (mRNA IP-ed / Lysate)
Vasa-IP	1080 ng ± 155. 24	37.6 %
eIF4E-IP	1081 ng ± 243. 66	37.6 %
Nanos2-IP	430 ng ± 163. 71	14.9 %
PreI-IP	470 ng ± 173. 49	16..4 %
Lysate	2870 ng ± 686. 36	-

C

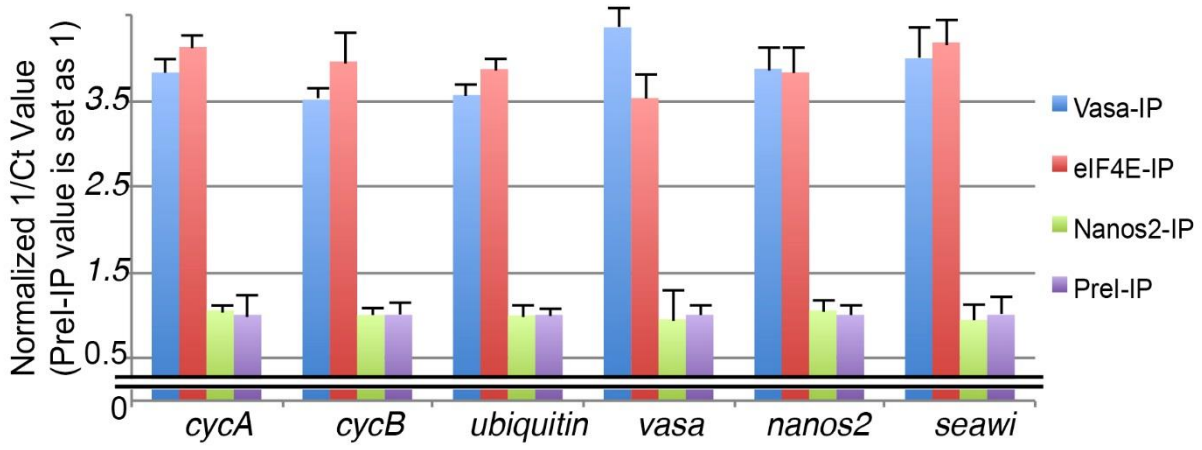

Figure S5, related to Figure 3. Vasa RNA-IP identified a broad range of mRNAs that interacted with Vasa. **A,** The 4-8cell stage embryos were lysed either at M-phase or S-phase. The Vasa interacting mRNAs were Immunoprecipitated (IPed) by Vasa antibody (Vasa-IP) and run on the agarose gel with mRNAs IPed with Pre-immune IgG beads (PreI-IP, negative control), together with lysate. Vasa attracted a large number of RNAs, whereas Pre-immune IgG pulled down reduced amount of RNA IPed in the same experimental condition. **B,** The total amount of RNAs IP-ed with each antibody-beads from 4-8 cell M-phase embryonic lysate is listed. **C,** The same proportion of each IP-ed sample was subjected to RT-qPCR. Vasa- and eIF4E-IPed samples demonstrated enrichment of the transcripts compared to the Nanos and PreImmune (PreI) pullouts. Each 1/Ct value of PreI samples is set as 1. Error bars indicate SD of three independent experiments.

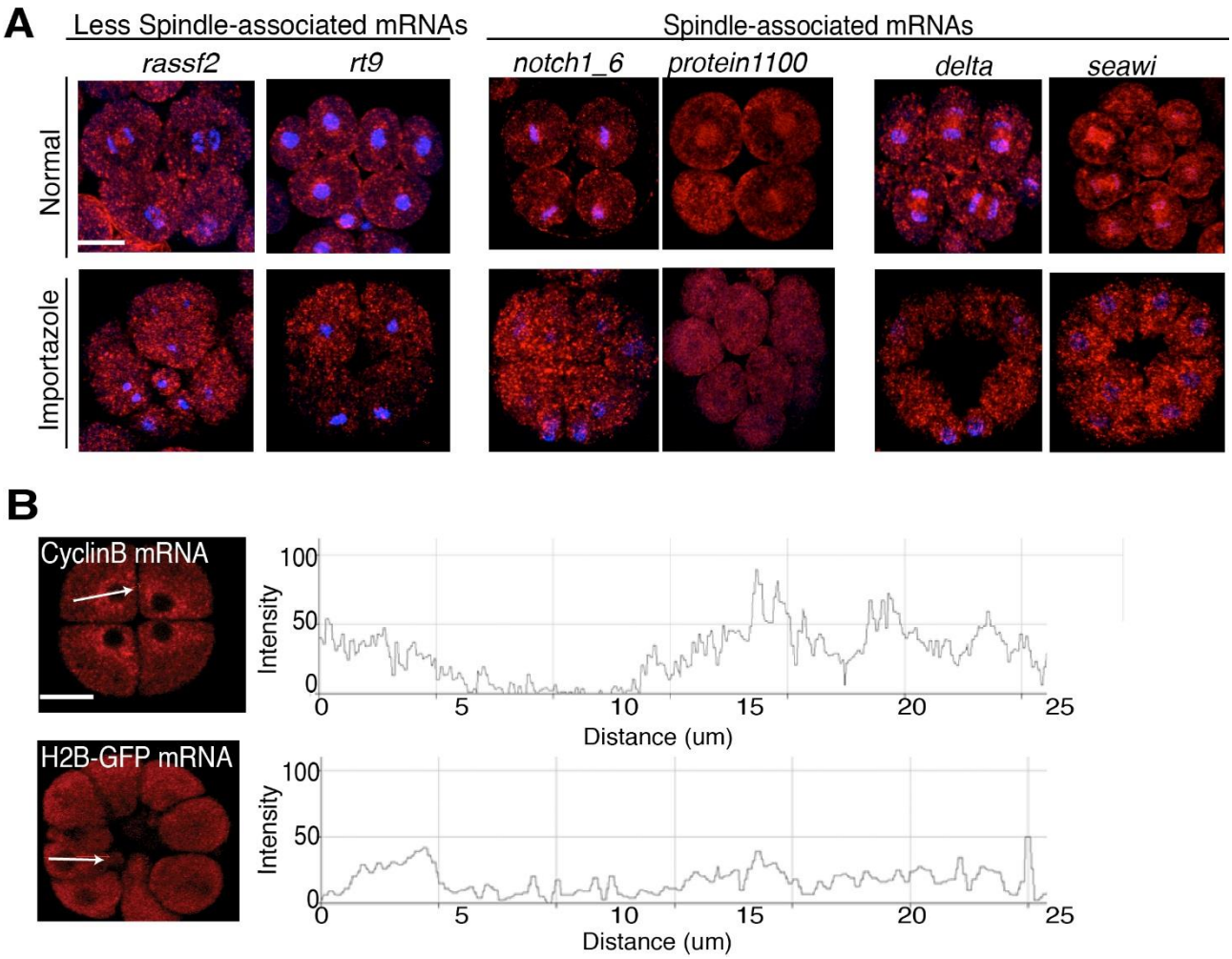

Figure S6, related to Figure 4. Importin is necessary for the mRNA localization in the embryo. Images were taken by confocal microscopy. **A,** Various mRNAs are localized around spindle and perinuclear during cell-cycling yet Importazole diminished their specific localization. Some mRNAs (*rassf2, rt9*) showed less enrichment, whereas the others (*notch1_6, protein1100, delta, seawi*) showed strong enrichment around the spindle and nuclear envelope. **B,** Intensity plot of *cyclinB* or *H2B-GFP* mRNA localization calculated by LSM5 Image Browser (Zeiss). The plot indicates the *cyclinB* mRNA is significantly accumulated around the nuclear envelope yet the *H2B-GFP* mRNA is rather evenly distributed throughout the cytoplasm. The mRNAs were labeled by Alexa546-UTP and injected into fertilized eggs. X-axis indicates the distance from the starting point of an arrow in each panel. Images were obtained at 8-16cell stage. Scale bars = 20 μm.

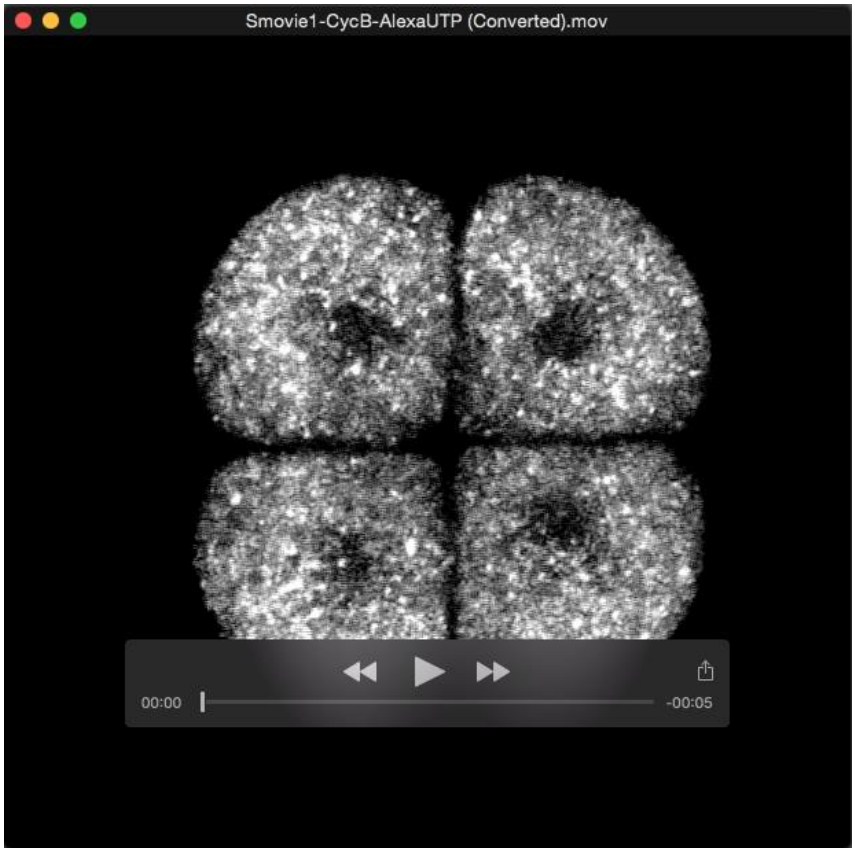

Movie S1, related to Figure 4. Dynamic distribution of CyclinB-mRNA. The time-lapse images were taken every 10min for 1hr. The movie (4fps) was constructed by *image J* software.

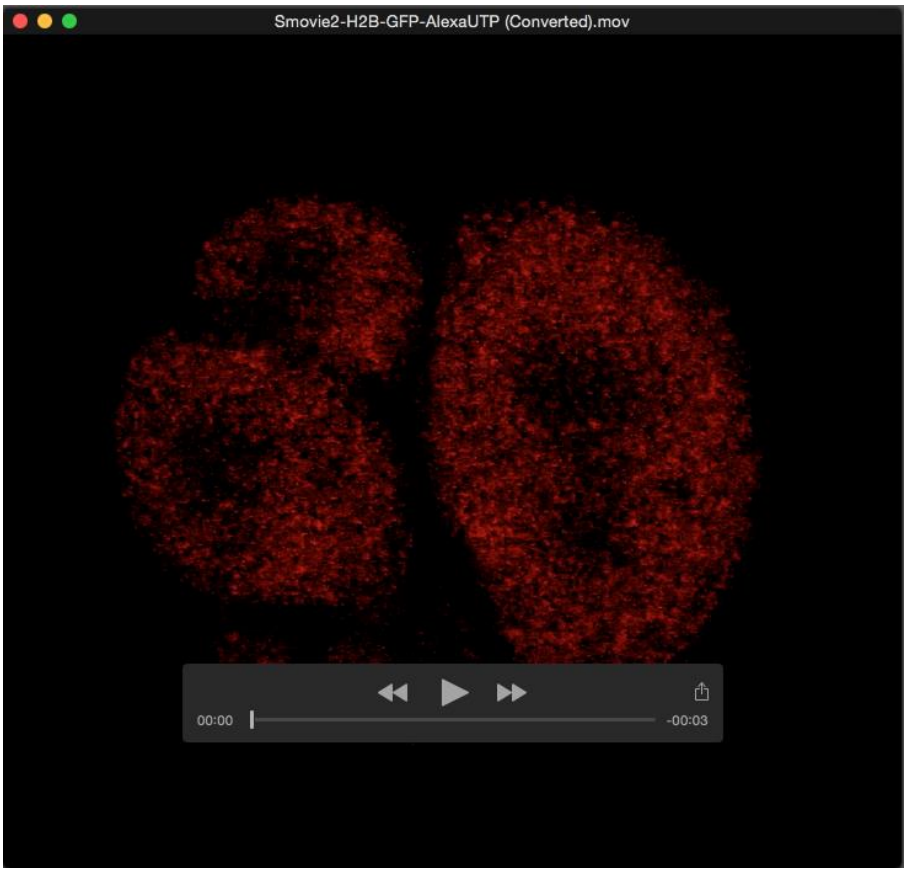

Movie S2, related to Figure 1. Even distribution of H2B-GFP mRNA. The time-lapse images were taken every 10min for 1hr. The movie (7fps) was constructed by *image J* software.

Supplementary Table 1, related to experimental procedure.

SPU #	Primer name	Primer Sequence
	Primers for in situ hybridization	
SPU_020907	*Sp-rassf2*	F: CCTTTACTTTGCTGGTTCAAGACC R: CTTGTCTTGCTGTTATAGAGATGCC
SPU_016539	*Sp-rt9*	F: GGTCCTTGAGAGGATTGTCACAGCTC R: CATGTCAAGATCAGGTAGCACACTG
SPU_007264	*Sp-notchh1_6*	F: GTGAATGGCTTTAGATGTGTCTGT CCCGAGGGTTA R: CATCAAAACCACTAGCACAGCTGCA CAGGTAAC
SPU_023939	*Sp-hypothetical protein-1100*	F: CATGACGAAAGGTCACACACAAAAC R: CGATGACCAGAGCTACCAGGAGACTC
SPU_016689	*Sp-seawi*	F: CACCAAGCATGGATCGTC R: GAAAAGAGAATACATGGTGTCC
SPU_008908	*Sp-vasa*	F: GGACGATCAACTAGCTTCTA R: ACTCCTTCGTCTTTCTTCAT
SPU_015614	*Sp-nanos2*	F: AAGGTGATGAGGGGAGGAAG R: CGCAAATCACCTGTACAAAAA
SPU_015285	*Sp-cyclinB*	F: GGCTTACACCAAGACCCAGA R: GAGGGATCGTATTGCACCAT
	Primers for ORF cloning	
SPU_015285	*Sp-cyclinB ORF (1.2kb)*	F: ATGGCTCATGCCACAAGAAACC R: CTACGATTCTTCCACTAGTGTC
	Primers for qPCR	
SPU_003528	*Sp-cyclinA*	F: GAGATTATCAAGGCCCAAAGG R: GTCTTGTTGCTCGTCTATTC
SPU_015285	*Sp-cyclinB*	F: CTGTAGTGAGTCTACCAGTG R: GCTGAGAAAATGCTTCAATG
SPU_021496	*Sp-ubiquitin*	F: CACAGGCAAGACCATCAC R: GAGAGAGTGCGACCATCC
SPU_008908	*Sp-vasa*	F: TCAACTACGACCTCCCAAGC R: TCTCGCAATGTTAGCATCCTT
SPU_021496	*Sp-seawi*	F: GTGATGGTGTTGGTGACAGC R: TATTGATGCGCTTCTTGACG
SPU_016128	*Sp-delta*	F: ACGGAGCTACATGCCTGAAC R: CTGCCAGTCTGTAGAAGGCTTC